Industria y Comercio
SUPERINTENDENCIA

Prosperidad para todos

SUPERINTENDENCIA DE INDUSTRIA Y COMERCIO

RAD: 13-138097- -2 **FECHA**: 2014-11-11 15:58:26
DEP: 2020 DIRECCION DE NUEVAS CREACIONES **EVE:** 1 REGISTRO/DEPOSITO/CONCESION/DEPOSITO
TRA: 2 PATENTES DE INVENCION **FOLIOS**: 6
ACT: 519 PRESENTACION

DIRECCIÓN DE NUEVAS CREACIONES

2020
Bogotá, D.C.,

Abogado(a)/Señor(a)
FELIPE EDUARDO FIGUEROA CARDOZO

Asunto: Radicación: 13-138097- -2
Trámite: 2
Evento: 1
Actuación: 519
Oficio: 14261
Folios: 6

Patente de Invención	**X**			Patente de Modelo de Utilidad	
Vía Nacional	**X**				
Vía PCT (Fase Nacional)		Capítulo I		Capítulo II	
No. Solicitud Internacional					
Fecha de Presentación Internacional					

Como resultado del examen de fondo realizado, con fundamento en el Artículo 45 de la Decisión 486 de la Comisión de la Comunidad Andina, se comunica:

1. Documentos estudiados

Descripción:	Radicado No 13-138097-00000-0000	07/Junio/2013
Reivindicaciones:	Radicado No 13-138097-00000-0000	07/Junio/2013
Dibujos	Radicado No 13-138097-00000-0000	07/Junio/2013

2. Análisis de la Prioridad

Se acepta la reivindicación de prioridad porque ésta solicitud fue presentada dentro del plazo establecido (Art. 9 D 486) y su contenido técnico corresponde con el de la prioridad reivindicada.

3. Objeto de la invención

De acuerdo con lo establecido en el numeral 1.2.2.2 del capítulo primero del Título 10 de la Circular Única para efectos del examen de patentabilidad, se tendrá en cuenta la tasa pagada por el solicitante al momento de comenzar el examen para las reivindicaciones adicionales; esto es que cuando la solicitud contenga más de diez (10)

reivindicaciones y no se haya pagado la tasa complementaria, sólo se estudiarán las cubiertas por la tasa pagada.

En el presente caso se estudiarán las reivindicaciones 1 a 3 (Radicado No 13-138097-00000-0000).

Título de la solicitud: “Complejos quitina - glucano y proceso para la preparación de los mismos a partir de biomateriales ricos en quitina”.

El problema planteado en esta solicitud consiste en la necesidad de proporcionar un proceso que permita la obtención de quitina y complejos quitina-glucano a partir de materias primas como micelio de microhongos y/o exoesqueletos de crustáceos que supere las dificultades en el manejo de efluentes contaminantes y en los que no se utilicen grandes cantidades de soluciones cáusticas o ácidas.

Para resolver este problema técnico la solicitud en estudio proporciona un proceso de obtención de un complejo de quitina-glucano y un complejo quitina-glucano, a partir de materias primas de origen biológico ricas en quitina como es el caso de microhongos y exoesqueletos de crustáceos mediante control del tamaño de partícula, mezcla con agua y un agente emulsificante no iónico, en donde la presión de operación es igual o superior a la presión de vapor de agua, luego se enfría la mezcla, se lava con el fin de remover proteínas y azúcares y se procede a recuperar y secar el sólido con un porcentaje de humedad inferior a 18%.

El objeto de la presente solicitud se relaciona con la Clasificación Internacional de Patentes (CIP): B05C 1/01.

4. De la solicitud de patente

Reivindicaciones (Art 30 D 486, Art 22 PCT)

1– El emulsificante de la reivindicación 1 solo está definido por su carácter químico al indicar la forma iónica en la que se encuentra y además no hay sustento para definir cualquiera que se encuentre en un rango de HLB entre 10 y 20. Se sugiere definirlo indicando el tipo de emulsificante utilizado en el procedimiento.
2– En la reivindicación 2 el término “opcionalmente” es imprecisa porque hace opcional a la característica y no limita el alcance de la reivindicación. Se sugiere reemplazarlo por un término preciso o rango concreto.
3– En la reivindicación 2 se mencionan múltiples opciones para la base empleada en el proceso y para las cuales no hay sustento en el capítulo descriptivo, lo cual no permite tener certeza de cuál fue la que se utilizó. Se sugiere indicar la base que tiene sustento en el capítulo descriptivo.
4- La reivindicación 3 reclama un producto a partir del proceso por el cual se obtuvo, se aclara que cuando se reivindica un producto, éste sólo puede ser definido en términos de su proceso de fabricación si: el producto es nuevo e inventivo y no se puede definir por sus características estructurales. Se sugiere definirlo por sus características esenciales.

5. Determinación del Estado de la Técnica

El estado de la técnica se determinó con base en la fecha de presentación de la solicitud de patente nacional: junio 7 de 2013, y se encontraron los siguientes documentos que anticipan el objeto de esta solicitud:

Ítem	Documento	Título	Fecha de Publicación*
D1	Department of Chemical	“Conversion of Crab Shell to	05/Octubre/2007

Ítem	Documento	Título	Fecha de Publicación*
	Engineering, Osaka Prefecture University, Sakai, Japan, Hidemi Nakamura, Hiroki Oozono, Norihisa Nakai and Hiroyuki Hidemi Nakamura, Hiroki Oozono, Norihisa Nakai and Hiroyuki Yoshida	Usefull Resources Using Sub critical water treatment"	
D2	Food Byophisics Vol. 4 (Pág. 213-228). C. Kriegel K.	"Influence of surfactant type and concentration on electrospinning of chitosan-poly/Ethylene oxide blend Nanofibers"	24/Junio/2009

El documento D1[1] divulga un método para preparar quitina, quitosan a partir de conchas de cangrejo empleando el tratamiento de agua subcrítica, que comprende proveer al sistema de material biológico, pulverizarlo, calentarlo a una temperatura comprendida entre 533K -563K por 1-10 min, extraer el material sólido obtenido y llevarlo a un análisis por HPLC (Pág. 1, Fig.1). El documento también divulga la adición de NaOH a la mezcla (Pág. 1)

El documento D2[2] divulga un método para preparar soluciones de polímeros como el quitosan que comprende: adicionar un surfactante no iónico Brij 35 en una proporción 0.01, 0,09 y 2mM a la solución (Pág. 215).

6. Examen de Patentabilidad (Art 14 D486)

Nivel inventivo (Art18 D486)

La reivindicación 1 consiste en *"Proceso para la preparación de complejos quitina-glucano o quitosano a partir de materias primas de origen biológico ricas en quitina, que comprende las etapas de: a) lavar el biomaterial seleccionado de micelio de microhongos o exoesqueletos de crustáceos hasta pH neutro, secar hasta alcanzar humedad relativa inferior a 20% y disminuir el tamaño de partícula, donde más del 90% de las partículas presentan un diámetro promedio menor o igual a 1mm (…)"*

Comparación de las características técnicas esenciales, con las del estado de la técnica:

Características esenciales	D1	D2
Proceso para la preparación de complejos quitina-glucano a partir de origen biológico, que comprende:	Método para preparar quitina, quitosán a partir de conchas de cangrejo que comprende:	Método para preparar soluciones de polímeros como el quitosán que comprende:
Lavar el biomaterial seleccionado de micelio de hongos o exoesqueleto de crustáceos, secar, disminuir el tamaño de la partícula a un diámetro de 1mm.	Macerar las conchas de cangrejo hasta pulverizarlas. (Pág. 1)	
Mezclar a temperatura ambiente el biomaterial en una proporción entre 10% y 30%, agua entre 70% y 90% y un agente emulsificante no iónico en una proporción entre 0.01 y 1% y HBL entre 10 y 20	-	Adición de un surfactante no iónico Brij 35 en una proporción 0.01, 0,09 y 2mM a la solución (Pág. 215).
Calentar la mezcla a una temperatura entre 100 y 370 °C, por un tiempo entre 0.1 y 50 segundos.	Calentar la mezcla a una temperatura entre 533K -563K por 1-10 min.(Pág. 1, Fig.1)	

11 http://www.esi.nagoya-u.ac.jp/h/isets07/Contents/Session05/1318Nakamura.pdf

22http://download.springer.com.ezproxy.unal.edu.co/static/pdf/554/art%253A10.1007%252Fs002890050021.pdf?auth66=1415131904_a265c98785c50c8b8a0023c5b932b742&ext=.pdf

2 http://www.esi.nagoya-u.ac.jp/h/isets07/Contents/ISETS07_TentativeProgram_20071005.pdf

Características esenciales	D1	D2
Enfriar la mezcla hasta una temperatura entre 35 y 30 en un tiempo entre 0.1 y 30 segundos.	Enfriamiento de la mezcla.	
Lavar con agua para remover proteínas y azúcares y recuperar el sólido.	El sólido es separado de la solución acuosa y llevado a un filtro (Pág. 2)	
Secar el sólido hasta lograr un porcentaje de humedad inferior al 18%.	Sólido seco (Pág. 2)	

El documento D1 se consideran el estado de la técnica cercano a la invención definida en la reivindicación 1 porque divulga un método para preparar quitina, quitosan y oligosacáridos a partir de conchas de cangrejo empleando el tratamiento de agua subcritica, que comprende proveer al sistema de material biológico, pulverizarlo, calentarlo a una temperatura comprendida entre 533°K -563°K por 1-10 min, extraer el material sólido obtenido y llevarlo a un análisis por HPLC (Pág. 1, Fig.1). El documento también divulga la adición de NaOH a la mezcla (Pág. 1). El documento también divulga que el producto obtenido contiene quitina y quitosan (Pág. 1).

El documento D2 divulga un método para preparar soluciones de polímeros como el quitosan que comprende: la adición de un surfactante no iónico a la solución (Pág. 215). El documento también divulga que las concentraciones del surfactante aniónico como el Brij 35 es 0.01, 0,09 y 2mM (Pág. 215). El documento también divulga que el producto obtenido es una mezcla de nanofibras que contienen quitosan (Pág. 215).

La diferencia consiste en que la solicitud divulga la adición de un agente emulsificante no iónico en una proporción entre 0.01 y 1%.

El efecto que logra adicionar un surfactante no iónico es estabilizar la suspensión.

Por lo tanto, el problema técnico objetivo que pretende resolver esta invención se puede formular así: cómo proporcionar un método para producir una emulsión de complejo quitosan-glucano estable.

Sin embargo, la utilización de surfactantes en un proceso para producir soluciones de polímeros como el quitosan, ya está divulgada en el documento D2 que se refiere al efecto de los surfactantes no iónicos sobre las propiedades de las soluciones tales como la viscosidad, la tensión superficial y la conductividad. El uso de surfactantes tienen aplicación en procesos de disolución de polímeros en técnicas de fluidos supercríticos [3] y específicamente surfactantes no iónicos favorecen la interacción polímero-surfactante [4].

En consecuencia, la persona del oficio normalmente versada en la materia, incluiría un surfactante de carácter no iónico sugerido en el documento D2 en el procedimiento divulgado en el documento D1 para llegar así al objeto de la reivindicación 1 de la solicitud. Por lo cual se considera obvia.

Las reivindicaciones dependientes 2-3 no mencionan características técnicas adicionales por lo cual tampoco tienen nivel inventivo.

---

3 3Biomedical exploitation of chitin and chitosan via mechano-chemical disassembly, electrospinnig, dissolution in imidazolium ionic liquids, and supercritical drying (1510-1533) http://www.mdpi.com/1660-3397/9/9/1510

4Effect surfactant concntration, pH and shear rateo n the rheological properties of aquos systems of a hydrophobically modifed chitosan and its unmodified analogue (71-79) http://link.springer.com/article/10.1007%2Fs002890050021#page-1

En conclusión, la reivindicación 1 cumple el requisito de novedad (Art. 16), pero no cumple con el requisito de nivel inventivo (Art. 18).

7. Conclusión

Los requisitos de patentabilidad de la presente solicitud están afectados así:

Ítem	Documento	Reivindicaciones afectadas	Requisito que afecta
D1	Department of Chemical Engineering, Osaka Prefecture University, Sakai, Japan, Hidemi Nakamura, Hiroki Oozono, Norihisa Nakai and Hiroyuki Hidemi Nakamura, Hiroki Oozono, Norihisa Nakai and Hiroyuki Yoshida	1-3	Nivel Inventivo
D2	Food Byophisics Vol. 4 (Pág. 213-228). C. Kriegel K.	1-3	Nivel Inventivo

En cumplimiento del artículo 45 de la Decisión 486 de la Comisión de la Comunidad Andina, se le indica que debe dar respuesta dentro del término de sesenta (60) días contados a partir del día siguiente de la fecha de notificación de la presente comunicación. En caso de no dar respuesta al presente requerimiento, o si a pesar de la respuesta subsistieran los impedimentos para la concesión, se denegará la patente.

Se invita al solicitante se sirva indicar, si así lo considera, su renuncia al término faltante de sesenta (60) días para dar respuesta a este requerimiento y presentarla por escrito.

Finalmente, se le recuerda al solicitante que si como respuesta a este requerimiento llegara a modificar el capítulo reivindicatorio y éste contenga más de diez (10) reivindicaciones, no pagará la tasa de modificación voluntaria pero sí la correspondiente al pago por reivindicación adicional.

Notifíquese el presente oficio conforme a lo dispuesto en el numeral 5.2, literal e), del capítulo quinto del título primero de la Circular Única No. 10 de 2001.

JESUS FERNEL GARCÍA GARCÍA
Director de Nuevas Creaciones (E)

El anterior requerimiento fue notificado por fijación en lista, de fecha 2014-11-18

Elaboró: Edna Milena Bautista Rodriguez
Revisó: Consuelo Leguizamon Leguizamon

SUPERINTENDENCIA DE INDUSTRIA Y COMERCIO
CONSULTA DE DOCUMENTOS

Food Biophysics (2009) 4:213–228
DOI 10.1007/s11483-009-9119-6

ORIGINAL ARTICLE

Influence of Surfactant Type and Concentration on Electrospinning of Chitosan–Poly(Ethylene Oxide) Blend Nanofibers

C. Kriegel · K. M. Kit · D. J. McClements · J. Weiss

Received: 31 October 2008 / Accepted: 15 June 2009 / Published online: 24 June 2009

Abstract Electrospun blend nanofibers were fabricated from chitosan (1,000 kDa, 80% DDA) and poly(ethylene oxide) (PEO; 900 kDa) at a ratio of 3:1 dispersed in 50% and 90% acetic acid. The influence of surfactants on the production of electrospun nanofibers was investigated by adding nonionic polyoxyethylene glycol dodecyl ether (Brij 35), anionic sodium dodecyl sulfate, or cationic dodecyl trimethyl ammonium bromide below, at, and above their specific critical micellar concentration to the polymer blend solution. Viscosity, conductivity, and surface tension of polymer solutions, as well as morphology and composition, of nanofibers containing surfactants were determined. Pure chitosan did not form fibers and was instead deposited as beads. Addition of PEO and an increasing concentration of surfactants induced spinnability and yielded larger fibers with diameters ranging from 10 to 240 nm. Surfactants affected morphology yielding needle-like, smooth, or beaded fibers. Compositional analysis revealed that nanofibers consisted of both polymers and surfactants with concentration of the constituents in nanofibers differing from that in polymer solutions. Results suggest that surfactants may modulate polymer–polymer interactions thus influencing the morphology and composition of deposited nanostructures.

Keywords Electrospinning · Chitosan · PEO · Surfactants

C. Kriegel
Northeastern University, Department of Pharmaceutical Sciences,
360 Huntington Avenue, 212 Mugar Life Science Building,
Boston, MA 02115, USA

D. J. McClements
Department of Food Science, Chenoweth Laboratory,
University of Massachusetts,
100 Holdsworth Way,
Amherst, MA 01003, USA

K. M. Kit
Department of Materials Science and Engineering,
University of Tennessee,
434 Dougherty Engineering Building,
Knoxville, TN 37996, USA

J. Weiss (✉)
Department of Food Science and Biotechnology,
University of Hohenheim,
Garbenstrasse 25,
70599 Stuttgart, Germany
e-mail: j.weiss@uni-hohenheim.de

Introduction

In electrospinning, ultrafine polymer nanofibers may be obtained by the application of a strong electrical field between a grounded target and a polymer solution that is pumped from a storage chamber through a small capillary orifice. Fibers are collected as a nonwoven mesh or membrane on a collector plate that acts as the counter electrode.[1,2] These fibers are of increasing interest to the food industries due to their potential application as novel packaging materials, membranes, or controlled release systems in ingredients.

To date, a wide variety of polymers have been electrospun with synthetic polymers yielding the best results. Biopolymers such as chitosan derived from agricultural raw materials and used in foods are of great interest because they may be nontoxic, edible and digestible, biocompatible and biodegradable, and renewable and sustainable, giving rise to a broader utilization especially in fields such as biomedical sciences, pharmaceuticals, cosmetics, and other related fields.[3–5] However, electrospinning of biopolymer solutions has proven to be difficult due their polycationic nature, low chain flexibility opposing chain entanglement, and poor solubility in organic solvents. In particular, the

repulsive interaction encountered in similarly charged polycationic chitosan chains may prevent sufficient chain entanglement required for continuous jet ejection and, therefore, fiber formation.

One approach to circumvent this problem has been to add cospinning agents such as salts or other polymers. These cospinning agents may either provide for additional entanglement and/or decrease electrostatic repulsive interactions. For example, chitosan has been electrospun from mixtures of chitosan and polymers that facilitate entanglement such as poly(vinyl alcohol),[6,7] poly(ethylene oxide) (PEO),[8,9] and others.[10] Pure chitosan has only been successfully electrospun from highly concentrated solutions of chitosans of relatively low molecular weight and/or in solvents such as trifluoroacetic acid,[11] 1,1,1,3,3,3-hexafluoro-2-propanol[12] where further purification and removal of the solvent from fibers was subsequently required.[13]

In this study, we suggest that addition of surfactants may be used to improve spinnability of solutions to yield natural nanofibers. Surfactants are amphiphilic molecules that readily absorb at surfaces and thereby lower surface or interfacial tension of the medium in which they are dissolved; a key parameter that influences electrospinning. Surfactants above a critical concentration self-assemble to form a variety of colloidal structures. These colloidal structures have different properties from those of the dissolved surfactant monomers, e.g., solubility, surface hydrophilicity, charge density. We further suggest that surfactants with charged headgroups may exhibit strong electrostatic interactions with charged biopolymers in the solution (e.g., chitosan). This may have a pronounced effect on solution properties, such as conductivity and surface tension, which in turn influences the occurrence of bending instabilities yielding fibers with different structures, thickness, and mechanical strength. For example, it has been reported that the addition of a small amount of nonionic surfactant to polymer solutions reduced the onset voltage required to induce spinnability and improved reproducibility of the electrospinning process.[14] Others found that, in systems of nonionic polymers, nonionic surfactants did not stop bead formation but greatly reduced it, while cationic surfactants prevented beaded fibers and led to fibers with smaller diameters.[15] In a previous study, we demonstrated that addition of nonionic surfactants to solutions of chitosan or chitosan–PEO blends improved fiber characteristics. When ionic micelles were added to these systems, conductivity was significantly improved and bead on string structures on the filaments were suppressed, allowing for the formation of smaller bead defect-free fibers.

Based on our previous studies and the above cited published literature, we hypothesize that addition of surfactants below, at, or above the critical micellar concentration significantly influences fiber morphologies of electrospun fibers since polymer–surfactant and subsequently polymer–polymer interactions are possibly altered. The objective of this study was, therefore, to determine the influence of surfactant type and concentration on solution properties, as well as morphologies and compositions of electrospun fibers from chitosan–PEO–surfactant solutions.

Materials and Methods

Materials

Chitosan with a medium molecular weight was obtained from Primex (Reykjavik, Iceland) in the form of flakes. As stated by the manufacturer, the viscosity in 1% acetic acid was 569 cP (M_w~1,000 kDa) and the degree of deacetylation was 80%. PEO (Cat. # 343) with a molecular weight of 900 kDa was purchased from Scientific Polymer Products (Ontario, NY, USA). Glacial acetic acid (CAS # 64197, UN 2789) was purchased from Acros Organics (Morris Plains, NJ, USA). Anionic sodium dodecyl sulfate (SDS; #71729) was obtained from Fluka, nonionic polyoxyethylene glycol (23) lauryl ether (Brij 35; #P1254) from Sigma, and cationic dodecyl trimethyl ammonium bromide (DTAB; CAS # 1119944) from Acros Organics (see above). The critical micellar concentrations were 2.3, 0.09, and 14 mM for SDS, Brij 35, and DTAB, respectively.[16] All reagents were used as received from the manufacturer without further purification.

Methods

Preparation of Polymer Solutions

Solutions were prepared with distilled and deionized water and reagent grade glacial acetic acid. Chitosan, PEO, and chitosan–PEO dispersions (3:1) at an overall polymer concentration of 1.6% (*w*/*w*) were prepared by dispersing chitosan and PEO in 50% and 90% acetic acid. Based on preliminary experiments on the electrospinnability of chitosan–PEO blend solutions, a 3:1 mass ratio of chitosan to PEO was selected. Solutions containing surfactants at three different concentrations below, at, and above the critical micellar concentration in water (0.01, 0.09, and 2 mM Brij 35; 10.9, 14, or 36 mM DTAB; 1, 2.3, and 10 mM SDS) were obtained by dissolving the surfactants first in distilled deionized water or acetic acid followed by dispersion of chitosan and PEO. Additional controls consisted of 0.4% PEO and of 1.2% chitosan—the concentrations of individual components used in the chitosan–PEO blend. Concentrations of all polymer solutions were expressed in percent weight per weight, except where noted otherwise. All the solutions were prepared

under constant magnetic stirring for a minimum of 8 h at 25 °C to ensure complete dissolution of the polymers. All solutions were then used immediately for electrospinning and analysis of solution properties.

Electrospinning

A previously described electrospinning setup was used.[17] Briefly, a syringe (Micro-Mate, Popper & Sons, New Hyde Park, NY, USA) fitted with a 0.69-mm diameter stainless steel capillary (No. 91019; Hamilton, NE, USA) with a blunt tip was filled with 20 mL of polymer solutions. The syringe was placed in a syringe pump (Harvard apparatus; 11plus, Holliston, MA, USA) which permitted adjustment and control of solution flow rates. The metal capillary of the syringe was connected to the positive lead of a high-voltage power supply (Gamma High Voltage; ES 30P-5W, Ormond Beach, FL, USA) operated in positive DC mode that could generate voltages up to 30 kV. A grounded copper plate wrapped in aluminum foil and mounted on two polypropylene blocks was used as the target for collection of fibers and/or beads. The target was placed 10 cm away from the capillary tip. The syringe pump delivered polymer solution at a controlled flow rate of 0.02 mL/min. The electrospinning was carried out at an applied voltage of 20 kV and a temperature at 25 °C. These conditions were kept constant throughout all experiments. Electrospun fiber mats were stored in desiccators prior to fiber characterization to prevent moisture uptake.

Solution Viscosity

Solution viscosity was measured with an oscillatory rheometer equipped with a double coaxial cup and bob measurement system (length=40 mm, diameter=26.66 mm, gap width=0.225 mm; MCR 300, Paar Physica, NJ, USA). The shear stress σ (in pascals) was recorded as a function of shear rate $\dot{\gamma}$ (per second) from 10^{-3} to 10^{3} s^{-1}. Solutions were equilibrated to 25 °C prior to all measurements using a Peltier system. Reported results are averages of triplicate measurements. Measurements were fitted to the power law model:[17]

$$\sigma = K\dot{\gamma}^{n} \tag{1}$$

where K is the consistency coefficient and n is the flow behavior index. If the flow behavior index n equals 1, the solution behaves as a Newtonian fluid; if the index n is smaller than 1, the solutions is a shear-thinning fluid; and if the index is larger than 1, the solution is a shear-thickening fluid.

Solution Conductivity

Electrical conductivity of the polymer solutions was determined using a Zetasizer (Nano series, Malvern Instruments, Worcestershire, UK). The temperature was adjusted to 25 °C prior to the measurements. Reported results are averages of triplicate measurements.

Surface Tension of Solutions

Surface tensions of solutions were determined using a digital tensiometer (Model K10ST, Kruss USA, Nazareth, PA, USA) based on the Wilhelmy plate method.[17] Forty grams of the tested solutions was poured into a 70-mm diameter glass beaker which had been previously rinsed with absolute ethanol and deionized and double-distilled water and dried at 70 °C overnight to remove any surface-active material. Solutions were then equilibrated to 25 °C and the platinum plate was lowered into the dispersion to form a meniscus. The surface tension σ was calculated in millinewtons per meter from the force F acting on the platinum plate using Eq. 2 where L is the length of the total meniscus (2×length + thickness of the plate) and θ is the contact angle:

$$\sigma = \frac{F}{L\cos\theta} \tag{2}$$

Results shown are averages of duplicate measurements and duplicate samples.

Electron Microscopy of Nanofibrous Structures

The morphology of electrospun nanofibers was observed with a field emission scanning electron microscope (FESEM 6320 FXV, JEOL, MA, USA) operating at 5 kV. Nanofibers were electrospun directly onto aluminum scanning electron microscope stubs which were mounted on the grounded collector plate. After collection of the fibers, samples were sputter coated with Au in a sputter coater (Model 108, Cressington, Watford, UK) for 60 s to reduce electron charging effects. Additional coatings were necessary for samples containing DTAB. The average fiber diameter was determined by image analysis (ImageJ, NIH, USA) from >50 randomly selected fibers for each sample.

Fourier Transform Infrared Spectroscopy

Compositional and chemical characteristics were evaluated by recording infrared spectra of electrospun fibers using a Fourier transform infrared (FTIR) spectrophotometer (Model IR Prestige 21, Shimadzu Corporation, Columbia, MD, USA) with an attenuated total reflection unit attached. Samples were mounted on the mirror and each specimen was scanned between 4,000 and 700 cm^{-1}. Each measurement consisted of an average of 32 scans at a resolution of 4 cm^{-1} using a Bessel apodization. IR-Solution (Shimadzu, Columbia, MD, USA) and Peakfit 4.12 (SeaSolve Soft-

ware, San Jose, CA, USA) were used to analyze and deconvolute infrared spectra.

Differential Scanning Calorimetry

Thermal analysis of electrospun fibers was carried out with a differential scanning calorimeter (Model Q100 DSC, TA Instruments, DA, USA). Samples of approximately 5 mg were loaded in DSC pans that were closed using a crimping tool. The specimens were equilibrated to 25 °C for 5 min and then heated from 25 to 180 °C at a heating rate of 2 °C/min. The temperatures of the sample and reference pans were measured as a function of oven temperatures to determine heat flows. Results represent an average of four measurements.

Statistical Analysis

All experiments were performed in duplicates or triplicates and repeated twice (see above). Data are expressed as the mean + standard deviations. Mean separations were determined using the Student's t test with a level of significance of $p<0.05$ (SAS Ver. 9.0, SAS Institute, Cary, NC).

Results and Discussion

Physical Properties of Composite Solutions

Conductivity

Electrical conductivity of 50% aqueous acetic acid was 0.98 mS/cm whereas that of 90% acetic acid was 0.03 mS/cm (Tables 1 and 2). At lower solvent concentrations, more molecules could be ionized and thus higher conductivities were observed. Pure PEO solutions had approximately the same conductivity as the solvents, i.e., 50% and 90% acetic acid. Conductivities of chitosan solutions were considerably higher than those of PEO and increased with increasing chitosan concentration, e.g., conductivities of 1.2% chitosan were 1.34 and 0.25 mS/cm in 50% and 90% acetic acid, respectively.

As PEO was added to the system, conductivity of chitosan–PEO solutions decreased compared to that of pure chitosan solution. This is because the solutions contain less of the polyionic polymer (chitosan) and more of the uncharged PEO. Solutions containing Brij 35 had conductivities ranging between 1.39–1.47 and 0.20–0.26 mS/cm in 50% and 90% acetic acid, respectively. With increasing concentration of Brij 35, the conductivities slightly decreased possibly due to Brij 35 interfering with the electron transport between electrodes. Generally, polymer dispersions containing 50% aqueous acetic acid had significantly higher conductivities compared to polymer dispersions in 90% acetic acid due to increased ionization. Conductivities of solutions containing SDS ranged from 1.43 to 1.63 mS/cm in 50% acetic acid, depending on SDS concentration, and 0.20, 0.22, and 0.38 mS/cm in 90% acetic acid for 1, 2.3, and 10 mM SDS, respectively. Conductivities of DTAB containing polymer dispersions were significantly higher than those containing either Brij or SDS, e.g., conductivities rose from 1.69 to 1.79 and 2.55 mS/cm for 10.9, 14, and 36 mM DTAB, respectively. When DTAB and chitosan–PEO were dispersed in 90% acetic acid, polymers were not completely dissolved; and no measurements could be performed on these samples. Moreover, in neat acetic acid, not enough polymers could be dissolved to allow for electrospinning.

Surface Tension

As acetic acid concentration increased from 50% to 90%, surface tension decreased from 38.6 to 30.8 mN/m without significant changes in viscosity (Tables 1 and 2). Upon addition of surfactant, a decrease in surface tension was observed. In 50% acetic acid, surface tension of samples containing 0.01, 0.09, and 2 mM Brij 35 were 38.7, 38.3, and 37.2 mN/m, respectively, while addition of 10.9, 14, or 36 mM DTAB resulted in a decrease from 38 to 37.7 and 36.9 mN/m, respectively, which was lower than the effect observed for Brij 35. SDS led to the most pronounced decline in surface tension in 50% acetic acid. When the anionic surfactant was used in the polymer blend, surface tensions of 37.7 to 34.8 and 29.0 mN/m were recorded for 1, 2.3, and 10 mM SDS, respectively. In 90% acetic acid, surface tensions were 30.4, 31.7, and 30.9 mN/m in solutions containing 0.01, 0.09, and 2 mM Brij 35, respectively, and 31.9, 30.7 and 31.8 mN/m in solutions containing 1, 2.3, and 10 mM SDS, respectively. It is interesting to note that the effect of acetic acid was more influential on the surface tension and that addition of surfactants only had a slight effect. Overall, the surface tension was significantly lower in samples containing 90% acetic acid compared to solutions containing 50% acetic acid.

Generally, surface tension has been suggested to be one of the most important solution properties in the electrospinning of chitosan.[13] Surface tension and conductivity have counteracting effects, that is, the decreased surface tension will result in a lower electric field strength required for jet initiation,[14] while the decreased conductivity will require a higher electric field strength. Furthermore, surface tension has a direct influence on the formation of beads and bead defects.[18]

Viscosity

The apparent viscosity of chitosan at a shear rate of 100 s^{-1} ($\eta_{a,100}$) increased from 0.56 to 1.15 Pa s when the chitosan

Table 1 Electrical conductivity in millisiemens per centimeter and surface tension in millinewtons per meter of polymer–surfactant solutions dispersed in 50% acetic acid

Samples in 50% acetic acid	Conductivity [mS/cm]	Surface tension [mN/m]
Acetic acid	0.98±0.00	38.55±0.07
1.2% chitosan	1.41±0.03	39.10±0.14
1.6% chitosan	1.64±0.03	37.95±0.07
0.4% PEO	0.99±0.01	38.80±0.00
1.6% PEO	0.93±0.01	38.65±0.07
Chitosan–PEO	1.40±0.03	37.80±0.00
Chitosan–PEO 0.01 mM Brij 35	1.47±0.02	38.65±0.07
Chitosan–PEO 0.09 mM Brij 35	1.39±0.04	38.30±0.14
Chitosan–PEO 2 mM Brij 35	1.39±0.02	37.20±0.35
Chitosan–PEO 1 mM SDS	1.43±0.02	37.70±0.14
Chitosan–PEO 2.3 mM SDS	1.48±0.02	34.75±0.64
Chitosan–PEO 10 mM SDS	1.63±0.02	29.00±0.00
Chitosan–PEO 10.9 mM DTAB	1.69±0.06	38.00±0.41
Chitosan–PEO 14 mM DTAB	1.79±0.05	37.65±0.17
Chitosan–PEO 36 mM DTAB	2.55±0.07	36.85±0.26

concentration increased from 1.2% to 1.6% in 50% acetic acid. The solvent itself had an apparent viscosity of 0.01 Pa s. In PEO solutions, an approximately 18-fold increase in apparent viscosity (from 0.01 to 0.18 Pa s) was observed when the polymer concentration was increased from 0.4% to 1.6%. The composite solution of PEO and chitosan had an apparent viscosity of 0.88 Pa s. While the addition of PEO decreased the viscosity of the solution, PEO has been successfully electrospun under a variety of conditions and thus is an ideal cospinning agent known to promote entanglement.[18–20]

With increasing concentrations of SDS (1, 2.3, and 10 mM) and Brij 35 (0.01, 0.09, and 2 mM), an increase in apparent viscosity from 0.85 to 0.92 Pa s and from 0.84 to 0.89 Pa s for SDS and Brij 35, respectively, of composite polymer solutions in 50% acetic acid was observed (Table 3). Table 3 also shows the results of a fit of the flow curve of polymer solutions measured at shear rates varying from 10^{-3} to 10^{3} s^{-1} to the power law (Eq. 1). From the fits, the power law consistency coefficient K and the power law flow behavior index n were determined. K increased from 5.42±0.65 to 13.04±0.32 when the concentration of SDS increased to 10 mM and from 7.81±0.26 to 9.63±0.29 when the concentration of Brij 35 increased to 2 mM. The flow behavior index n decreased significantly from 0.55±0.01 to 0.46±0.01 upon addition of 10 mM SDS. Addition of Brij on the other hand did not significantly impact the flow behavior index n (n=0.51± 0.01 at 0 mM Brij 35 and n=0.48±0.01 at 2 mM Brij 35). When DTAB was added to the polymer solutions, the apparent viscosity and K were slightly decreased from 0.90 to 0.83 Pa s and from 10.15±0.84 to 8.47±1.33, respectively. The flow behavior index n, however, remained virtually unchanged (0.48±0.01 versus 0.49±0.02).

The rheological properties of polymer solutions are indicative of a pronounced shear-thinning effect which

Table 2 Electrical conductivity in millisiemens per centimeter and surface tension in millinewtons per meter of polymer–surfactant solutions dispersed in 90% acetic acid

Samples in 90% acetic acid	Conductivity [mS/cm]	Surface tension [mN/m]
Acetic acid	0.03±0.01	30.75±0.07
1.2% chitosan	0.20±0.01	31.35±0.07
1.6% chitosan	0.30±0.02	31.90±0.00
0.4% PEO	0.03±0.01	30.40±0.00
1.6% PEO	0.03±0.01	30.50±0.00
Chitosan–PEO	0.16±0.01	31.88±0.13
Chitosan–PEO 0.01 mM Brij 35	0.26±0.02	30.45±0.31
Chitosan–PEO 0.09 mM Brij 35	0.22±0.02	31.70±0.60
Chitosan–PEO 2 mM Brij 35	0.20±0.01	30.90±0.74
Chitosan–PEO 1 mM SDS	0.20±0.01	31.93±1.01
Chitosan–PEO 2.3 mM SDS	0.22±0.02	30.68±1.53
Chitosan–PEO 10 mM SDS	0.37±0.02	31.80±0.18

Table 3 Apparent viscosity at a shear rate of 100 s^{-1} and power law indices K and n of chitosan–PEO–surfactant dispersions in systems containing 50% acetic acid as the solvent

Samples in 50% acetic acid	Apparent viscosity $\eta_{a,100}$ (Pa·s)	Power law consistency coefficient K	Power law flow behavior index n
Acetic acid	0.01±0.01	0.01±0.01	0.95±0.10
1.2% chitosan	0.56±0.01	4.90±0.11	0.52±0.01
1.6% chitosan	1.15±0.04	12.94±0.40	0.47±0.01
0.4% PEO	0.01±0.01	0.02±0.01	0.92±0.01
1.6% PEO	0.18±0.01	0.78±0.01	0.66±0.02
Chitosan–PEO	0.88±0.07	8.62±1.53	0.50±0.02
Chitosan–PEO 1 mM SDS	0.85±0.11	5.42±0.65	0.55±0.01
Chitosan–PEO 2.3 mM SDS	0.90±0.13	11.19±0.42	0.47±0.01
Chitosan–PEO 10 mM SDS	0.92±0.14	13.04±0.32	0.46±0.01
Chitosan–PEO 0.01 mM Brij 35	0.84±0.03	7.81±0.26	0.51±0.01
Chitosan–PEO 0.09 mM Brij 35	0.86±0.03	8.38±0.28	0.49±0.01
Chitosan–PEO 2 mM Brij 35	0.89±0.07	9.63±0.29	0.48±0.01
Chitosan–PEO 10.9 mM DTAB	0.90±0.01	10.15±0.84	0.48±0.01
Chitosan–PEO 14 mM DTAB	0.87±0.01	8.98±0.04	0.47±0.10
Chitosan–PEO 36 mM DTAB	0.83±0.05	8.47±1.33	0.49±0.01

can be related to polymer entanglement. Entanglement of polymers in the electrospinning solution is critical to the formation of fibers. If polymers are not or insufficiently entangled, beads or droplets instead of fibers are typically deposited on the collector plate due to the low viscoelastic force which does not counterbalance the higher Coulombic stretching force that causes jet instability.[8,12,13,21–26] The critical chain overlap concentration c^*, which is the crossover concentration between the dilute and the semidilute concentration regimes, is thus a critical parameter for electrospinning. The overlap concentration can be determined from the intrinsic viscosity as:[27]

$$c^* \sim [\eta]^{-1} \tag{3}$$

Gupta et al. studied the relationship between viscosity, polymer concentration, and fiber formation and found a good correlation between solution regimes and the occurrence of beads and droplets or bead defect-free and uniform fibers in electrospinning of poly(methyl methacrylate).[27] For example, polymer droplets together with beaded fibers were observed in the semidilute unentangled regime, at concentrations of $1<c/c^*<3$. However, polymer concentration had to be increased to $c\sim 6c^*$ for uniform fiber formation to occur with polymers of a narrow molecular weight distribution (MWD) and even higher concentrations were required in case of broad MWD. Thus, the extent of polymer entanglement depends on the polymer as well as the solvent and polymer concentrations needed to substantially exceed c^* for a successful electrospinning experiment

Table 4 Apparent viscosity at a shear rate of 100 s^{-1} and power law indices K and n of chitosan–PEO–surfactant dispersions in systems containing 90% acetic acid as the solvent

Samples in 90% acetic acid	Apparent viscosity $\eta_{a,100}$ (Pa·s)	Power law consistency coefficient K	Power law flow behavior index n
Acetic acid	0.01±0.01	0.01±0.01	1.01±0.01
1.2% chitosan	0.61±0.00	9.65±0.67	0.42±0.01
1.6% chitosan	1.15±0.06	14.50±0.16	0.44±0.01
0.4% PEO	0.02±0.00	0.01±0.00	0.88±0.01
1.6% PEO	0.27±0.01	1.46±0.14	0.63±0.01
Chitosan–PEO	1.04±0.04	12.70±1.70	0.44±0.02
Chitosan–PEO 1 mM SDS	1.17±0.12	14.24±2.12	0.45±0.02
Chitosan–PEO 2.3 mM SDS	1.07±0.08	14.41±1.55	0.43±0.01
Chitosan–PEO 10 mM SDS	1.07±0.11	14.54±2.80	0.32±0.17
Chitosan–PEO 0.01 mM Brij 35	1.30±0.00	13.10±0.11	0.45±0.01
Chitosan–PEO 0.09 mM Brij 35	1.05±0.00	14.72±2.26	0.45±0.01
Chitosan–PEO 2 mM Brij 35	0.99±0.06	14.50±0.10	0.43±0.01

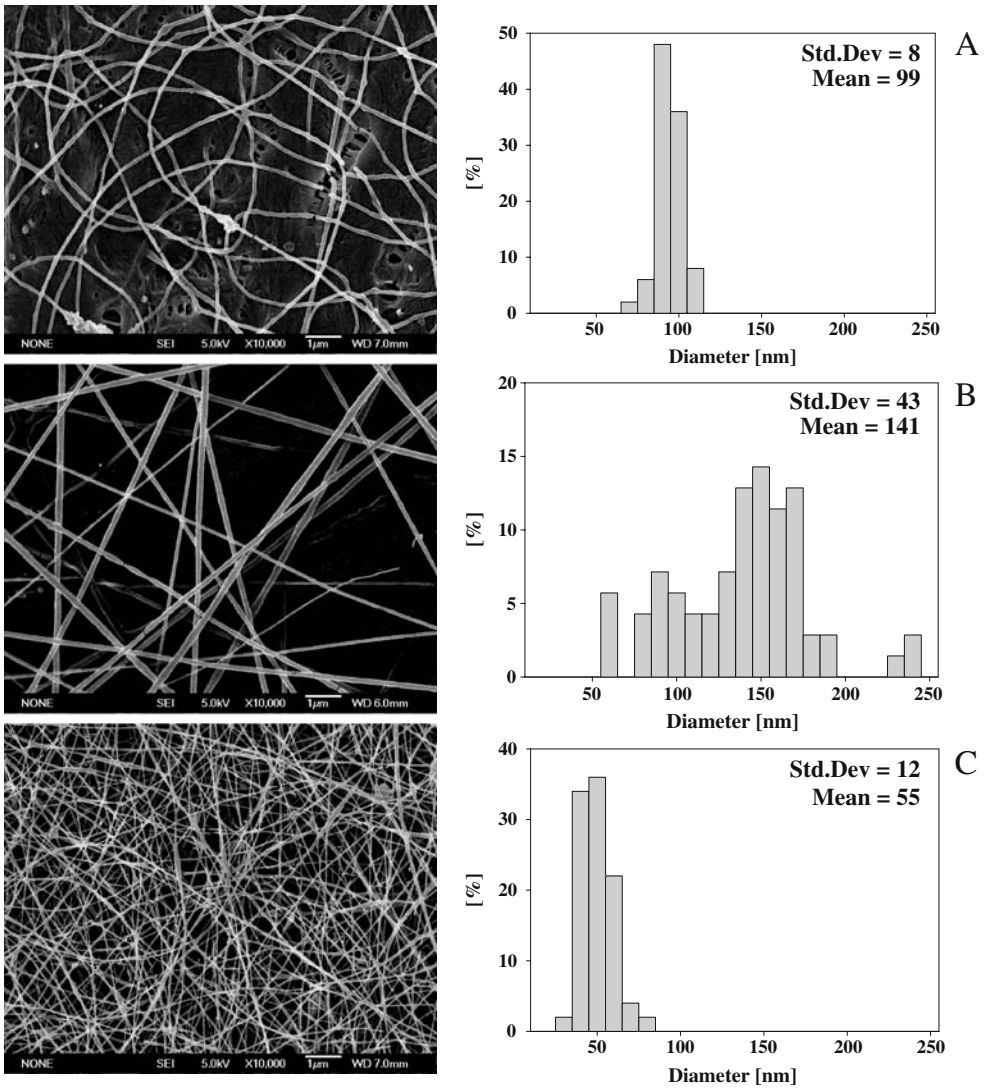

Fig. 1 Scanning electron microscopic images (magnification ×10,000) of depositions of electrospun polymer dispersions. **a** 1.6% PEO electrospun in 50% acetic acid; **b** 1.6% PEO in 90% acetic acid; **c** chitosan–PEO in 50% acetic acid; **d** chitosan–PEO in 90% acetic acid; chitosan–PEO with **e** 0.01 mM Brij 35, **f** 0.09 mM Brij 35, and **g** 2 mM Brij 35 in 90% acetic acid; chitosan–PEO with **h** 1 mM SDS, **i** 2.3 mM SDS, and **j** 10 mM SDS in 90% acetic acid; chitosan–PEO with **k** 2 mM Brij 35 in 50% acetic acid; chitosan–PEO with **l** 1 mM SDS in 50% acetic acid; as well as chitosan–PEO with **m** 10.9 mM DTAB, **n** 14 mM DTAB, and **o** 36 mM DTAB in 50% acetic acid

and nanofiber formation to occur. The critical chain overlap concentration in our system was previously determined to be 0.103 g/dL. Thus, we were working well above this critical concentration with c/c^* being >10.

A similar behavior was observed when 90% acetic acid was used as the solvent. Generally, viscosities of polymer blend solutions were higher using the more concentrated solvent. The apparent viscosity at a shear rate of 100 s^{-1} ($\eta_{a,100}$) increased from 0.61 to 1.15 Pa s in solutions containing 1.2% to 1.6% chitosan, respectively. The solvent had an apparent viscosity of 0.01 Pa s. One hundred percent PEO samples of 0.4% and 1.6% concentration dissolved in 90% acetic acid had apparent viscosities of 0.02 and 0.27 Pa s, respectively, while the composite solution had an apparent viscosity of 1.04 Pa s. Apparent viscosities decreased with increasing concentration of SDS or Brij 35 from 1.17 to 1.07 Pa s and from 1.30 to 0.99 Pa s, respectively. The consistency coefficient remained unchanged at 14.24±2.12 to 14.54±2.80 upon addition of SDS concentration and increased from 13.1±0.11 to 14.50±0.10 when increasing concentrations of Brij 35 were added. The flow behavior index n decreased for SDS-containing samples from 0.45±0.02 to 0.32±0.17 at 10 mM SDS but remained unchanged at 0.45±0.01 and 0.43±0.01 for 0 and 2.3 mM Brij 35, respectively. A flow index of 0.32 in SDS-containing solutions is indicative of a very strong shear-thinning behavior. Results of both viscosity and conductivity measurements highlight the strong influence that SDS appears to have on polymer–polymer interactions (Table 4).

Morphology and Fiber Diameter

Pure chitosan did not form fibers in either solvent. Instead, beads or drops with a very limited degree of fiber formation were deposited. Due to the limited solubility of chitosan in

Fig. 1 (continued)

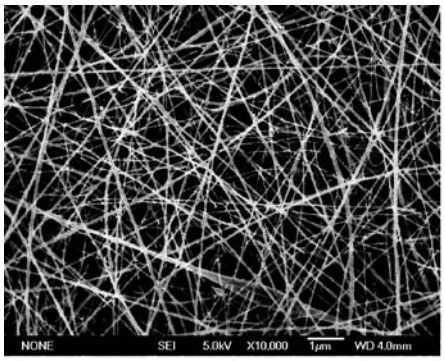

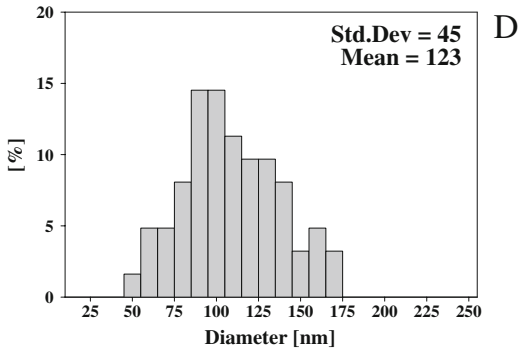

D

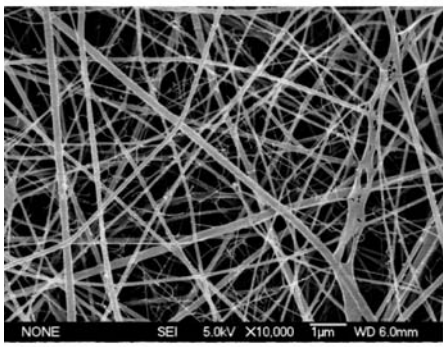

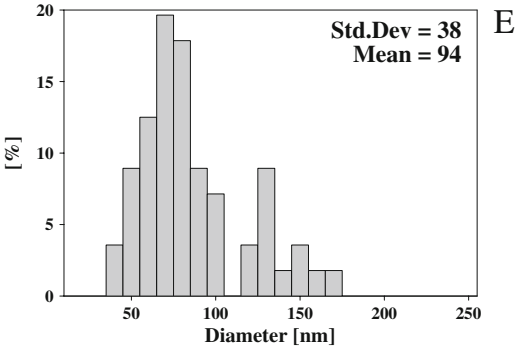

E

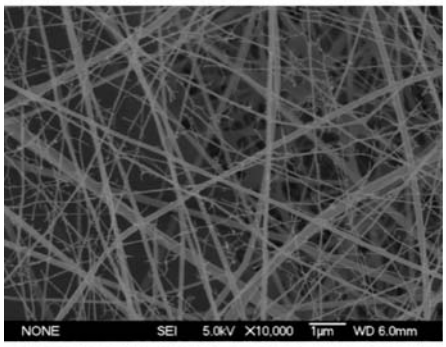

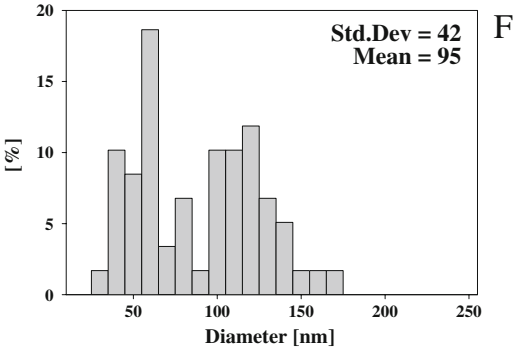

F

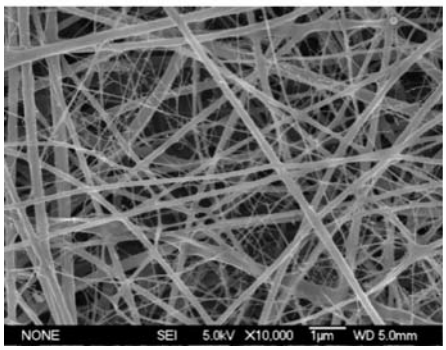

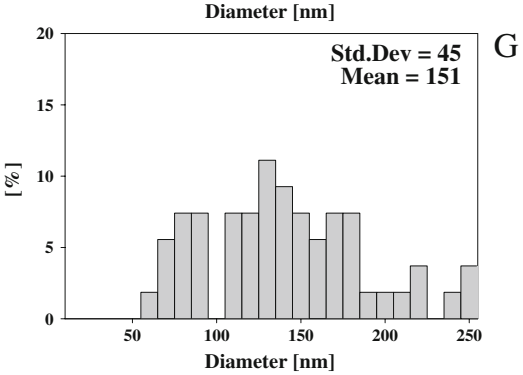

G

common organic solvents, the concentration of chitosan was likely too low to lead to a sufficiently high degree of entanglement required for electrospinning. Jets thus broke up into individual droplets instead of forming continuous fibers.

FESEM images showed that nanofibers had diameters ranging from of 10 to 250 nm. At 0.4 % PEO (the concentration of PEO in the composite solution), the solution was too diluted in either solvent to form continuous jets and only droplets were deposited. However, when the PEO concentration was increased to 1.6%, which equals the total polymer concentration in all the remaining samples, relatively uniform nanofibers were fabricated in 50% acetic acid with virtually no bead defects (Figure 1a). In 90% acetic acid, the fiber surfaces were smooth and fiber similarly lacked defects (Figure 1b). Fiber diameters ranged from 70 to 110 nm and from 60 to 240 nm for PEO fibers spun in 50% and 90% acetic acid, respectively. The

Fig. 1 (continued)

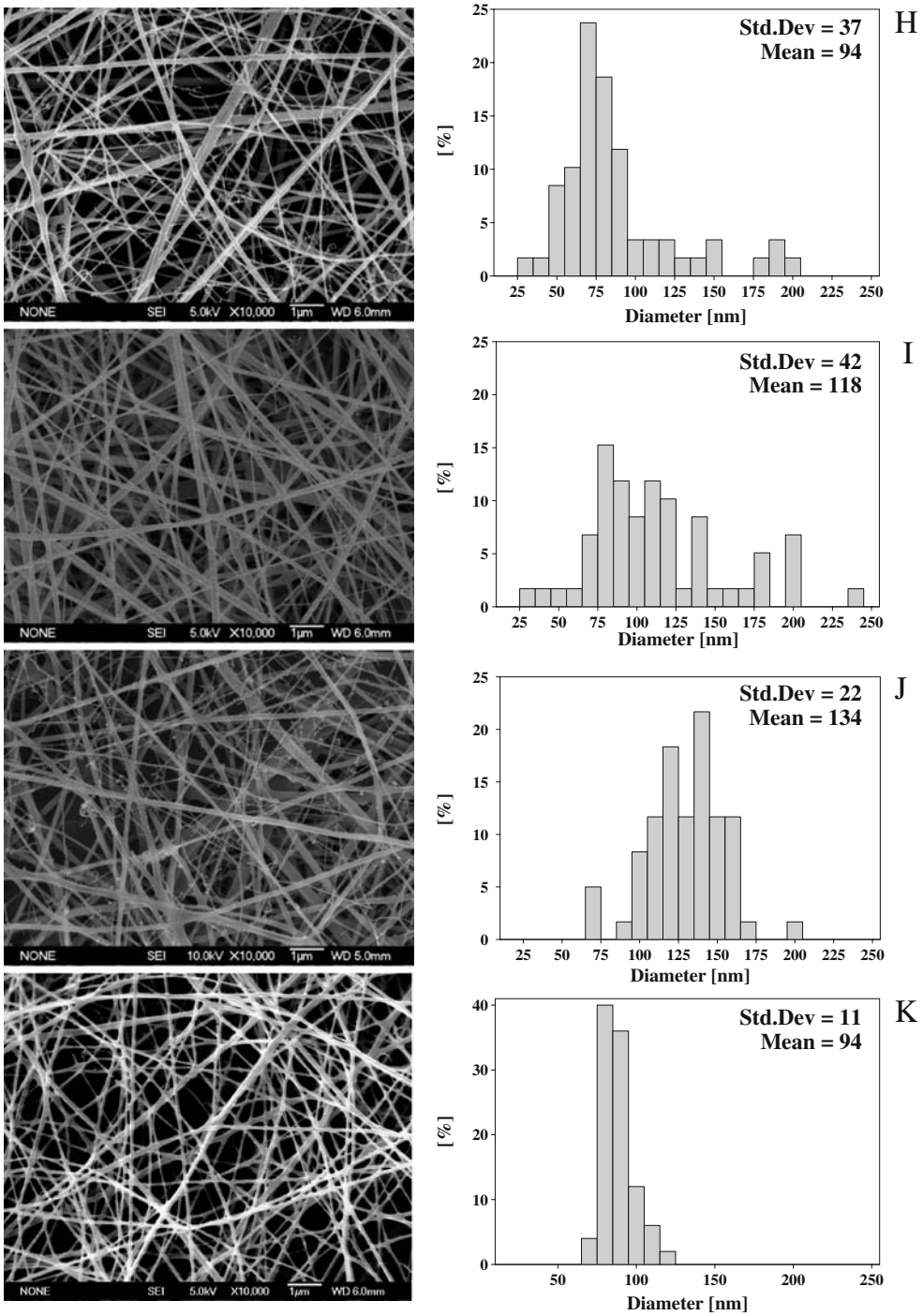

conductivity of the solution containing 50% acetic acid was higher compared to that of PEO in 90% acetic acid. The higher conductivity introduces more whipping and bending instabilities that yielded fibers with a smaller diameter and a somewhat rougher surface.

When chitosan was added to the PEO solution, the fiber diameter dramatically decreased to 30 to 80 nm in the case of 50% acetic acid and 50 to 170 nm in 90% acetic acid (Figure 1c, d). This may be attributed to an increased chitosan and a decreased PEO fraction in the solution. Amongst the tested acetic acid concentrations, 90% acetic acid appeared to be best suited to initiate electrospinning and form nanofibers without bead defects (Figure 1d–j). Bead defects can be an indication of inconsistent polymer flows. The flow rate and the strength of the applied electric field must both be properly adjusted so as to prevent that the supplied flow rate from the reservoir to the tip of the needle exceeds the flow rate of the polymer jet. Otherwise,

Fig. 1 (continued)

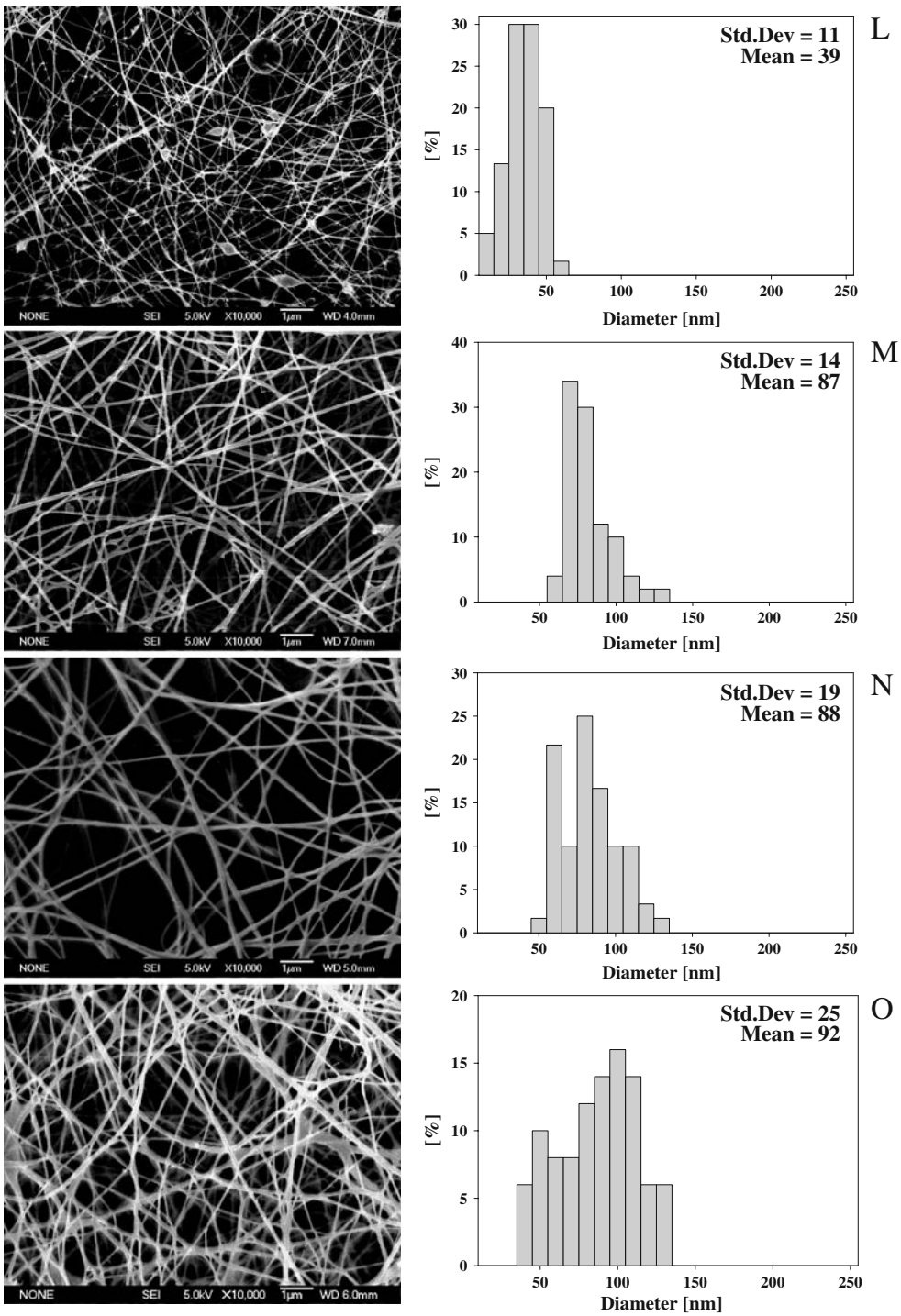

excess polymer solution will accumulate at the tip of the capillary and form a droplet that will eventually detach from the tip of the capillary to interrupt the continuous flow of the jet. On the other hand, if too little solution is supplied, the solution at the tip of the capillary will be depleted causing an interruption of the ejection of a polymer jet.

When Brij 35 was added to the polymer solutions, a sufficiently high amount of nonionic surfactant had to be added in order to initiate continuous fiber production. At insufficient concentrations of Brij, numerous bead defects and few small fibers were observed. For example, at 0 mM Brij, numerous bead defects were observed, while at 0.09 mM Brij, the number of bead defects decreased and more fibers with larger diameters were formed. At a concentration of 2 mM Brij 35, smooth nanofibers with diameters of 70 to 120 nm were deposited on the collector plate (Figure 1k). Long and branched fibers were observed,

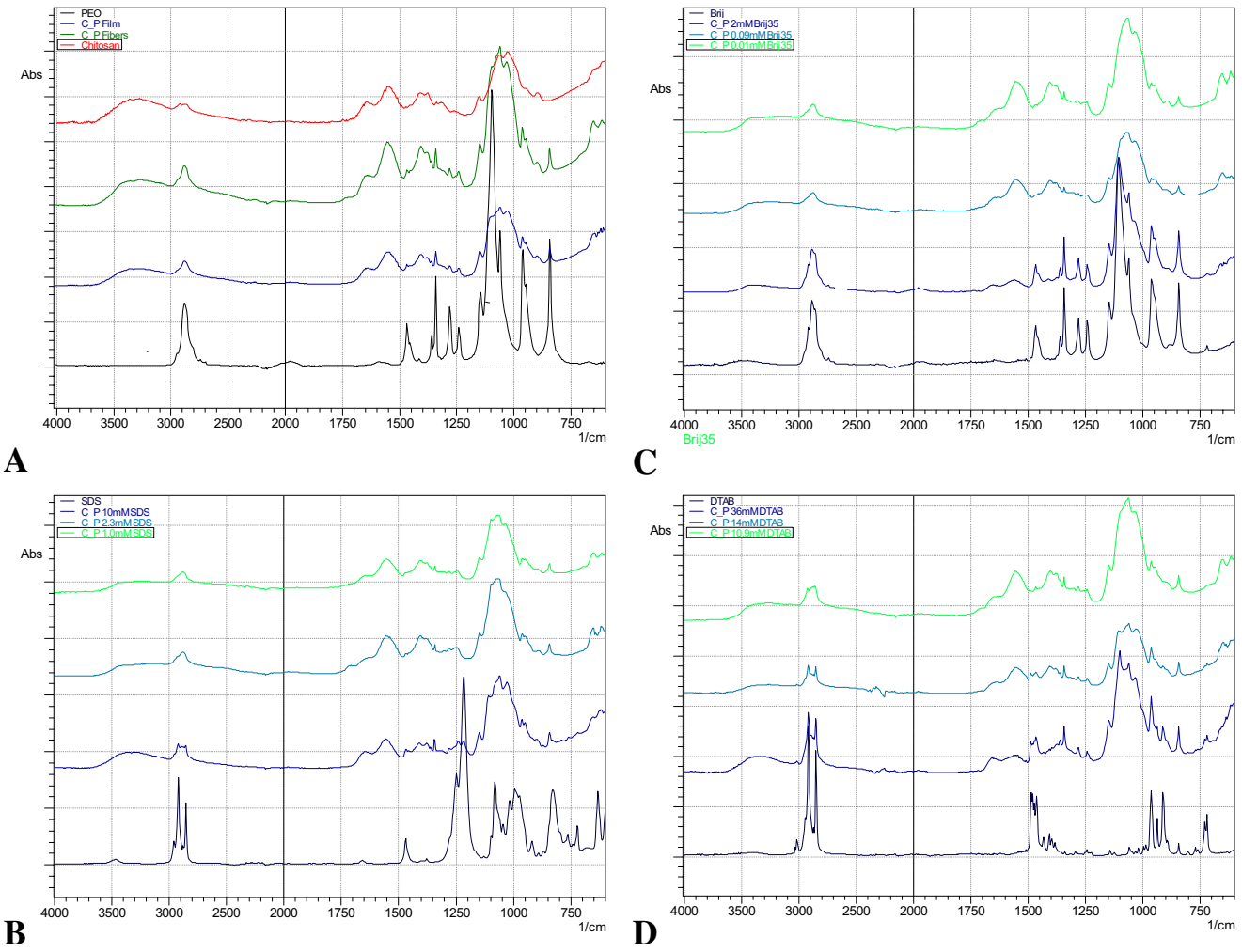

Fig. 2 Infrared absorbance spectra of electrospun chitosan–PEO–surfactant fibers at wave numbers ranging from 4,000 to 700 cm^{-1}. **a** Spectra of PEO (*1*), chitosan–PEO film (*2*), chitosan–PEO nanofibers (*3*), and chitosan powder (*4*); **b** spectra of pure Brij 35 powder (*1*), composite fibers with 2 mM (*2*), 0.09 mM (*3*), and 0.01 mM Brij 35 (*4*); **c** spectra of pure SDS powder (*1*) and composite nanofibers incorporating 10 mM (*2*), 2.3 mM (*3*), and 1 mM SDS (*4*); **d** spectra of pure surfactant powder of DTAB (*1*) as well as chitosan–PEO nanofibers containing 36 mM (*2*), 14 mM (*3*), and 10.9 mM DTAB (*4*)

which is indicative of the split of a single fiber during the electrospinning process. Addition of 1 mM SDS yielded nanofibers of 10–60 nm, the smallest size of nanofibers that was collected in these sets of experiments, and some bead defects were observed (Figure 1l). The smaller diameters can be associated with an increased charge density along the polymer jet, which can lead to higher elongational forces stretching the polymer jet. Increasing the concentration of the anionic surfactant to 2.3 mM drastically increased the number and size of bead defects, but at the same time, reduced the amount of fibers and their size. When 10 mM SDS was incorporated in the polymer solutions, no fiber formation was observed and only beads or drops were deposited. Nanofibers were formed from all polymer dispersions supplemented with DTAB independent of the concentration (Figure 1m–o). The average fiber size did not significantly vary among the three samples and fiber diameter ranged from 40 to 130 nm. The changes in the macroscopic appearances of the collected material are especially noteworthy. Nanofibers containing DTAB, the cationic surfactant, formed open, low-density networks comparable to spider webs rather than the dense paper-like deposition observed with all other surfactants.

Using 90% acetic acid, nanofibers were formed in polymer dispersions supplemented with Brij 35 or SDS regardless of the surfactant concentration. However, addition of DTAB led to the inability to dissolve the polymers in the solution; and polymers instead remained as dispersed powders. The viscosity of the solution was similar to that of the solvent, a further indication that polymers did not dissolve. Thus, nanofiber production was not possible at all. However, when the water content was increased (50% acetic acid), polymers could be dissolved and an increase in viscosity and polymer entanglement was seen. Addition of

up to 0.09 mM Brij 35 resulted in nanofibers having diameters ranging from 40 to 170 nm, while nanofibers produced from polymer solutions containing 2 mM Brij 35 had a broader diameter (60–250 nm).

Solutions containing 1 mM SDS produced fibers with sizes ranging from 30 to 200 nm. The diameter distribution was very broad, but fibers had very smooth surfaces. Higher concentrations of SDS caused an increase in fiber diameter. When 2.3 mM SDS was added, the diameter ranged from 30 to 220 nm. At 10 mM SDS, fibers had average diameters of 70–200 nm.

Compositional Analysis

Fourier Transform Infrared Spectroscopy

The infrared spectra of cast films and electrospun nanofibers are shown in Figure 2. Spectra of pure chitosan were obtained by analyzing solution cast films prepared in the same solvents used for electrospinning followed by drying overnight under vacuum to obtain a transparent polymer film. This is because chitosan could not be spun into fibers. The most characteristic absorption bands for chitosan consisted of a broad band at 3,400–3,100 cm^{-1}, which can be attributed to N–H and OH···O stretching vibration and intermolecular hydrogen bonding of the polysaccharide molecules,[6,28–30] and two strong bands at 1,655 and 1,550 cm^{-1} attributed to the carbonyl C=O–NHR or amide I band and the amine $–NH_2$ or amide II absorption band, respectively.[8,28,29]

Typical absorption bands for PEO can be detected at 2,885 cm^{-1} attributed to CH_2 stretching,[31] which can overlap with the band observed in chitosan samples. Other characteristic bands are observed at 1,470 cm^{-1} assigned to CH bending, at 1,340 cm^{-1} assigned to CH deformation of the methyl group, and absorption bands around 1,100 cm^{-1} assigned to C–O–C stretching vibration.[8] Since PEO with a high molecular weight (900 kDa) was used in the experiments, the OH absorption bands may be neglected. The OH absorption band in the range of 3,400 and 3,100 cm^{-1} is thus only attributed to OH within chitosan.[32] With the addition of PEO, the absorbance intensity of CH_2 stretching at 2,885 cm^{-1} increased while the absorbance intensity of $–NH_2$ stretching at around 1,550 cm^{-1} decreased.

PEO and the nonionic surfactant Brij 35 experience similar structural features as evidenced by similar FTIR spectra and absorption bands. Typical bands for DTAB include two strong absorption bands at 2,915 and 2,850 cm^{-1} attributed to CH_2 methylene stretching vibrations and four medium strong peaks in the range of 1,488 to 1,462 cm^{-1}. In case of SDS, characteristic bands are observed at 2,930, 2,847, 1,469, and 1,184 cm^{-1} assigned to symmetric CH stretching, asymmetric CH stretching, CH bending, and SO stretching, respectively. Generally, with increasing content of surfactant of any kind, the CH_2 stretching vibration around 2,900 cm^{-1} as well as bands characteristic for each specific surfactant increased (in case of DTAB at 1,500, 960, and 842 cm^{-1}) while bands typical for chitosan polysaccharide such as amide bands at 1,655 and 1,550 cm^{-1} gradually decreased, indicating that the content of chitosan decreased relative to the other components, suggesting that chitosan is less preferential ejected from the polymer surface.

Deconvolution of the FTIR spectra using single-component spectra of pure chitosan, PEO, Brij 35, SDS, and DTAB and calculation of peak areas by integration was used to determine the composition of nanofibers (IR-Solution, Shimadzu, Columbia, MD, USA and Peakfit

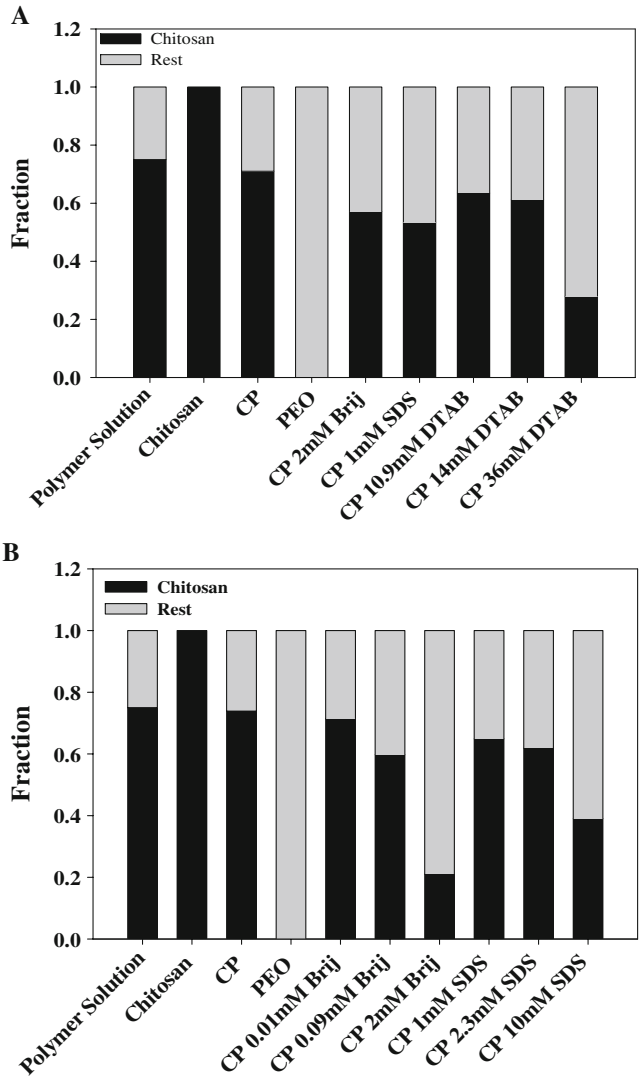

Fig. 3 Compositional analysis of composite nanofibers. **a** Composition of samples obtained in 50% acetic acid, **b** composition of samples spun in 90% acetic acid. Concentrations were calculated from analysis of infrared absorbance peaks at 1,550 cm^{-1}

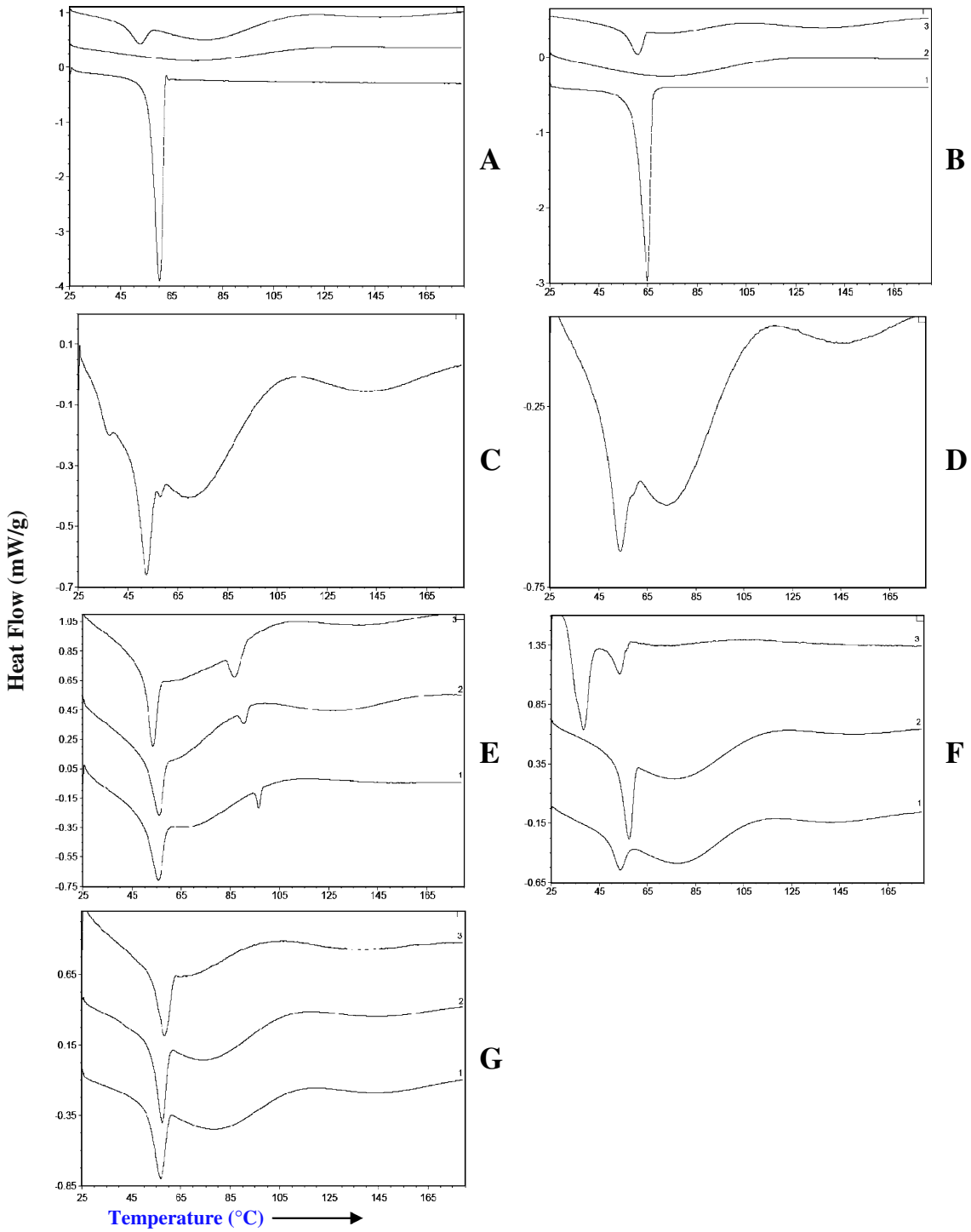

Fig. 4 Thermograms of electrospun composite fibers measured at a scanning rate of 2 °C/min from 25 to 180 °C. **a** Thermograms of chitosan–PEO fibers (*3*), chitosan powder (*2*), and PEO fibers (*1*) in 50% acetic acid; **b** thermograms of chitosan–PEO fibers (*3*), chitosan powder (*2*), and PEO fibers (*1*) in 90% acetic acid; **c** thermograms of composite nanofibers containing 2 mM Brij electrospun in 50% acetic acid, **d** fibers with 1 mM SDS solubilized in 90% acetic acid prior to nanofiber manufacture, and **e** nanofibers incorporating DTAB at 10.9 mM (*1*), 14 mM (*2*), and 36 mM (*3*); **f** thermograms of nanofibers with Brij 35 at 0.01 mM (*1*), 0.09 mM (*2*), and 2 mM Brij 35 (*3*) and **g** composite nanofibers with SDS of 1 mM (*1*), 2.3 mM (*2*), and 10 mM SDS (*3*)

Table 5 Heat flow data of nanofibers of chitosan–PEO–surfactant systems in 50% acetic acid

Samples in 50% acetic acid	T_m (°C)	$T_{m,2}$ (°C)	$T_{m,3}$ (°C)	$H_{m,1}$ (J/g)	$H_{m,2}$ (J/g)	$H_{m,3}$ (J/g)
Chitosan	82.23±3.50			291.58±15.93		
PEO	60.09±0.57			185.53±18.29		
Chitosan–PEO	52.34±0.25	81.93±1.94		26.22±0.74	109.75±11.34	
Chitosan–PEO 2 mM Brij 35	36.56±0.27	50.76±1.10	74.56±2.16	0.62±0.33	29.75±0.65	70.72±4.69
Chitosan–PEO 1 mM SDS	54.64±1.10	76.26±2.83		24.58±3.95	43.38±10.24	
Chitosan–PEO 10.9 mM DTAB	56.08±0.89	96.48±0.15		31.25±5.69	2.93±0.42	
Chitosan–PEO 14 mM DTAB	54.52±1.20	87.02±4.69		32.44±3.85	2.77±0.81	
Chitosan–PEO 36 mM DTAB	53.41±0.01	87.86±1.54		26.17±2.25	14.57±0.88	

Thermograms of electrospun composite fibers were measured at a scanning rate of 2 °C/min at a temperature range of 25 to 180 °C

4.12, SeaSolve Software, San Jose, CA, USA). Intensities at 1,550 cm^{-1} were used to calculate relative concentrations of chitosan in the nanodepositions (Figure 3). Chitosan concentration in electrospun nanofibers was 71% when 50% acetic acid was used and 73.9% when 90% acetic acid was used. These data were in close agreement of data obtained from thermogravimetric analysis (data not shown). Here, chitosan concentration was determined to be 75% in 90% acetic acid and 72% in 50% acetic acid. When Brij 35 was added to the solution to be electrospun, chitosan concentration in the fibers decreased to 57.1% using 50% acetic acid and from 71.5 to 21% with increasing surfactant concentration in 90% acetic acid. A similar trend was observed for the other two surfactants. Addition of SDS to the polymer dispersions in 50% acetic acid resulted in a decrease of the chitosan concentration to 53.5% and to 39% chitosan 90% acetic acid at the highest concentration of the anionic surfactant (10 mM). Using the cationic DTAB as an additive, the chitosan concentration decreased from 63.5% to 28% upon an increase in surfactant concentration from 10.9 to 14 and 36 mM. Thus, generally less chitosan was present in electrospun nanofibers upon addition of surfactants, a possible indication of a disruption of the wrapping entanglement of PEO with chitosan.

Thermal Analysis

DSC thermograms of fibers are shown in Figure 4 with analysis of thermograms shown in Tables 5 and 6. Pure chitosan powder, pure PEO electrospun nanofibers, as well as pure surfactant powders were used as controls in the DSC experiments. The majority of polysaccharides including chitosan do not experience melting but rather degradation upon heating above a certain temperature. This is due to their extensive associations through hydrogen bonding. Thus, rather than showing sharp transitions, their thermograms have broad endotherms with associated water evaporation below the degradation temperature.[8]

In the DSC thermogram of chitosan films prepared with 90% acetic acid, a broad peak was observed at 75.92± 1.90 °C. A similar broad peak also appeared in the thermogram of chitosan–PEO at a slightly higher temperature of 78.46±3.50 °C. A second peak was observed in the composite samples from PEO at 60.65±0.43 °C which represents a shift to a lower temperature from its original melting point at 64.71±0.76 °C in samples of pure PEO fibers. The peak temperature determined for the PEO film in 90% acetic acid was 65.27 °C±0.26 °C, which is somewhat higher than the melting point for PEO fibers, suggesting that the

Table 6 Heat flow data of nanofibers of chitosan–PEO–surfactant systems in 90% acetic acid

Samples in 90% acetic acid	$T_{m,1}$ (°C)	$T_{m,2}$ (°C)	$H_{m,1}$ (J/g)	$H_{m,2}$ (J/g)
Chitosan	75.91±1.90		248.46±6.23	
PEO	64.71±0.76		135.96±9.74	
Chitosan–PEO	60.65±0.43	78.46±3.50	23.59±2.71	21.60±3.24
Chitosan–PEO 0.01 mM Brij 35	53.57±0.74	80.59±0.04	15.80±1.48	70.28±6.01
Chitosan–PEO 0.09 mM Brij 35	57.74±0.93	81.65±0.32	27.97±5.83	54.98±21.15
Chitosan–PEO 2 mM Brij 35	37.92±0.58	51.93±1.20	64.40±5.66	20.29±3.71
Chitosan–PEO 1 mM SDS	57.22±0.84	79.43±2.57	36.43±2.27	52.09±6.87
Chitosan–PEO 2.3 mM SDS	56.63±0.12	86.42±1.24	31.88±2.29	84.59±5.00
Chitosan–PEO 10 mM SDS	57.16±1.07	75.17±3.02	33.66±2.04	35.12±5.05

Thermograms of electrospun composite fibers were measured at a scanning rate of 2 °C/min at a temperature range of 25 to 180 °C

overall crystallinity of PEO fibers is lower than in cast films. This can be associated with the electrically forced orientation of the polymer chains during electrospinning,[20] transforming the coiled polymer chains into oriented entangled structures, which are also present in the solidified electrodepositions. The melting point of PEO is even lower in the composite fibers, possibly due to interactions between PEO and chitosan chains obstructing the crystallization of PEO.

When 50% acetic acid was used to dissolve the polymers, a broad transition peak was observed at 82.23±3.50 °C for pure chitosan film, a sharp and intense peak at 60.09±0.57 °C for melting of pure PEO fiber, and a T_m at 52.34±0.25 and 81.93±1.94 °C in the composite fiber. The melting point of PEO in the PEO film was 65.35±0.27 °C. Using 50% acetic acid as the solvent caused an even more pronounced shift towards lower melting temperatures of PEO in both pure and composite fibers, which may correlate to a low crystallinity of PEO in these samples. This observation is of particular importance to possible applications of electrospun nanofibers.

Upon addition of increasing concentrations of the nonionic surfactant Brij 35 using 90% acetic acid as a solvent, the melting point for PEO and chitosan shifted from 53.57±0.74 and 80.59±0.04 °C at the lowest concentration of surfactant (0.01 mM Brij 35) for PEO and chitosan, respectively, to 57.74±0.93 and 81.65±0.32 °C at 0.09 mM Brij 35. A broad transition peak of chitosan was observed in both cases. When 2 mM Brij 35 was present in the polymer dispersion, the endotherm from chitosan decreased significantly compared to the other two endothermic melting transitions at 37.92±0.58 and 51.93±1.20 °C were observed in Brij 35 and PEO, respectively. Pure Brij 35 powder had two melting endotherms at 36.56±0.54 and 139.25±1.60 °C.

Increasing the concentration of the anionic surfactant SDS resulted in a shift of PEO and the broad chitosan endotherms from 57.22±0.84 and 79.43±2.57 °C at 1 mM SDS to 56.63±0.12 and 86.42±1.24 °C at 2.3 mM SDS to 57.16±1.07 and 75.17±3.02 °C at 10 mM SDS. Pure SDS had melt transitions at 99.76±0.10 and 106.35±0.44 °C.

Fibers containing 2 mM Brij 35 electrospun in 50% acetic acid had melting temperatures of 36.56±0.27, 50.76±1.10, as well as 74.56±2.16 °C, which may be attributed to Brij 35, PEO, and chitosan, respectively. Here, the melting point for PEO was reduced compared to fibers spun in 90% acetic acid. In the case of the anionic surfactant, only the lowest concentration of SDS yielded electrodepositions in 50% acetic acid. Here, T_m for both components shifted to lower transition temperatures when compared with the system produced in 90% acetic acid, e.g., 54.64±1.10 and 76.26±2.83 °C for PEO and chitosan, respectively.

When the cationic DTAB was added to the test system and 50% acetic acid was used as the solvent, two sharp peaks were present. The melting point of PEO was 56.08±0.89, 54.52±1.20, and 53.41±0.01 °C when the concentration of DTAB was increased to 36 mM. A second peak was observed at 96.48±0.15, 87.05±4.68, and 87.86±1.54 °C at a concentration of 10.9, 14, and 36 mM DTAB, respectively. Pure DTAB had a transition at 99.1±0.31 °C.

Conclusions

Ultrafine fibers could not be formed via electrospinning from chitosan solutions in 50 and 90 wt.% acetic acid. Instead, beads were deposited on the collector plate. However, fibers with diameters ranging from 10 to 240 nm were obtained from composite dispersions at a chitosan–PEO ratio of 3:1. When nonionic, anionic, and cationic surfactants were added to the polymer blend, smooth fibers of various sizes were obtained. Composite solutions containing DTAB at 90 wt.% acetic acid were not electrospinnable due to insufficient solubility. Measurement of solution properties such as viscosity, conductivity, and surface tension revealed that the polymer–solvent and polymer–polymer interactions are key factors in the electrospinning process and results suggest that surfactants are able to modulate these interactions via electrostatic and/or hydrophobic interactions as well as hydrogen bonding.

The obtained results are relevant to the food and agricultural industries due to the fact that they offer a new means to produce nanofibers that are solely or partially composed of food biopolymers and that are, therefore, suitable for use in food or food packaging. Rather than using organic solvents that are not suitable for food applications, food-approved emulsifiers may be used to induce electrospinning in solutions of biopolymer–polymer blend solutions. Food-grade nanofibers could find use in a wide variety of food applications ranging from packaging materials to filtration aids and new ingredients systems due to their unique properties.

Acknowledgements This work was supported by the Environmental Protection Agency Star Grant Program (grant number GR832372) and the Massachusetts Experiment Station supported by the Cooperative State Research, Extension, Education Service, United States Department of Agriculture, Massachusetts Agricultural Experiment Station (project nos. 831 and 911).

References

1. C. Burger, B.S. Hsiao, B. Chu, Annu. Rev. Mater. Res. **36**, 333–368 (2006). doi:10.1146/annurev.matsci.36.011205.123537
2. Z.M. Huang, Y.Z. Zhang, M. Kotaki, S. Ramakrishna, Compos. Sci. Technol. **63**(15), 2223–2253 (2003). doi:10.1016/S0266-3538(03)00178-7

3. M. Kumar, R.A.A. Muzzarelli, C. Muzzarelli, H. Sashiwa, A.J. Domb, Chem. Rev. **104**(12), 6017–6084 (2004). doi:10.1021/cr030441b
4. R.A.A. Muzzarelli, *Chitin* (Pergamon, Oxford, 1977)
5. H.K. No, S.P. Meyers, W. Prinyawiwatkul, Z. Xu, J. Food Sci. **72** (5), R87–R100 (2007). doi:10.1111/j.1750-3841.2007.00383.x
6. L. Li, Y.L. Hsieh, Carbohydr. Res. **341**(3), 374–381 (2006). doi:10.1016/j.carres.2005.11.028
7. Y.T. Jia, J. Gong, X.H. Gu, H.Y. Kim, J. Dong, X.Y. Shen, Carbohydr. Polym. **67**(3), 403–409 (2007). doi:10.1016/j.carbpol.2006.06.010
8. B. Duan, C.H. Dong, X.Y. Yuan, K.D. Yao, J. Biomater. Sci. Polym. Ed. **15**(6), 797–811 (2004). doi:10.1163/156856204774196171
9. A. Subramanian, H.-Y. Lin, D. Vu, G. Larsen, Biomed. Sci. Instrum. **40**, 117–122 (2004)
10. K.H. Jung, M.W. Huh, W. Meng et al., J. Appl. Polym. Sci. **105** (5), 2816–2823 (2007). doi:10.1002/app.25594
11. K. Ohkawa, K.I. Minato, G. Kumagai, S. Hayashi, H. Yamamoto, Biomacromolecules **7**(11), 3291–3294 (2006). doi:10.1021/bm0604395
12. B.M. Min, S.W. Lee, J.N. Lim et al., Polymer (Guildf.) **45**(21), 7137–7142 (2004). doi:10.1016/j.polymer.2004.08.048
13. X.Y. Geng, O.H. Kwon, J.H. Jang, Biomaterials **26**(27), 5427–5432 (2005). doi:10.1016/j.biomaterials.2005.01.066
14. L. Yao, T.W. Haas, A. Guiseppi-Elie, G.L. Bowlin, D.G. Simpson, G.E. Wnek, Chem. Mater. **15**(9), 1860–1864 (2003). doi:10.1021/cm0210795
15. T. Lin, H.X. Wang, H.M. Wang, X.G. Wang, Nanotechnology **15** (9), 1375–1381 (2004). doi:10.1088/0957-4484/15/9/044
16. A. Helenius, D.R. McCaslin, E. Fries, C. Tanford, Methods Enzymol. **56**, 734–749 (1979). doi:10.1016/0076-6879(79)56066-2
17. S. Wongsasulak, K.M. Kit, D.J. McClements, T. Yoovidhya, J. Weiss, Polymer (Guildf.) **48**(2), 448–457 (2007). doi:10.1016/j.polymer.2006.11.025
18. H. Fong, I. Chun, D.H. Reneker, Polymer (Guildf.) **40**(16), 4585–4592 (1999). doi:10.1016/S0032-3861(99)00068-3
19. Y.M. Shin, M.M. Hohman, M.P. Brenner, G.C. Rutledge, Polymer (Guildf.) **42**(25), 9955–9967 (2001). doi:10.1016/S0032-3861(01)00540-7
20. J.M. Deitzel, J. Kleinmeyer, D. Harris, N.C.B. Tan, Polymer (Guildf.) **42**(1), 261–272 (2001). doi:10.1016/S0032-3861(00)00250-0
21. N. Bhattarai, M.Q. Zhang, Nanotechnology **18**(45), 455601.1–455601.10 (2007). doi:10.1088/0957-4484/18/45/455601
22. H.L. Jiang, D.F. Fang, B.S. Hsiao, B. Chu, W.L. Chen, Biomacromolecules **5**(2), 326–333 (2004). doi:10.1021/bm034345w
23. M. Spasova, N. Manolova, D. Paneva, L. Rashkov, Preparation of chitosan-containing nanofibres by electrospinning of chitosan/poly (ethylene oxide) blend solutions. e-Polymers, Art. No. 056. (2004)
24. J.B. Xie, Y.L. Hsieh, J. Mater. Sci. **38**(10), 2125–2133 (2003). doi:10.1023/A:1023763727747
25. L.F. Zhang, Y.L. Hsieh, Carbohydr. Polym. **71**(2), 196–207 (2008). doi:10.1016/j.carbpol.2007.05.031
26. Y.S. Zhou, D.Z. Yang, J. Nie, J. Appl. Polym. Sci. **102**(6), 5692–5697 (2006). doi:10.1002/app.25068
27. P. Gupta, C. Elkins, T.E. Long, G.L. Wilkes, Polymer (Guildf.) **46** (13), 4799–4810 (2005)
28. Y. Wan, H. Wu, A.X. Yu, D.J. Wen, Biomacromolecules **7**(4), 1362–1372 (2006). doi:10.1021/bm0600825
29. C.L. De Vasconcelos, P.M. Bezerril, D.E.S. dos Santos, T.N.C. Dantas, M.R. Pereira, J.L.C. Fonseca, Biomacromolecules **7**(4), 1245–1252 (2006). doi:10.1021/bm050963w
30. Y. Hu, Y.M. Du, J.H. Yang, Y.F. Tang, J. Li, X.Y. Wang, Polymer (Guildf.) **48**(11), 3098–3106 (2007). doi:10.1016/j.polymer.2007.03.063
31. S. Zivanovic, J.J. Li, P.M. Davidson, K. Kit, Biomacromolecules **8**, 1505–1510 (2007). doi:10.1021/bm061140p
32. C. Sawatari, T. Kondo, Macromolecules **32**(6), 1949–1955 (1999). doi:10.1021/ma980900o

Mar. Drugs **2011**, *9*, 1510-1533; doi:10.3390/md9091510

OPEN ACCESS

Marine Drugs

ISSN 1660-3397

www.mdpi.com/journal/marinedrugs

Review

Biomedical Exploitation of Chitin and Chitosan via Mechano-Chemical Disassembly, Electrospinning, Dissolution in Imidazolium Ionic Liquids, and Supercritical Drying

Riccardo A. A. Muzzarelli

University of Ancona, IT-60100 Ancona, Italy; E-Mail: Muzzarelli.raa@gmail.it;
Tel./Fax: +39-071-36206.

Received: 26 July 2011; in revised form: 28 August 2011 / Accepted: 31 August 2011 / Published: 9 September 2011

Abstract: Recently developed technology permits to optimize simultaneously surface area, porosity, density, rigidity and surface morphology of chitin-derived materials of biomedical interest. Safe and ecofriendly disassembly of chitin has superseded the dangerous acid hydrolysis and provides higher yields and scaling-up possibilities: the chitosan nanofibrils are finding applications in reinforced bone scaffolds and composite dressings for dermal wounds. Electrospun chitosan nanofibers, in the form of biocompatible thin mats and non-wovens, are being actively studied: composites of gelatin + chitosan + polyurethane have been proposed for cardiac valves and for nerve conduits; fibers are also manufactured from electrospun particles that self-assemble during subsequent freeze-drying. Ionic liquids (salts of alkylated imidazolium) are suitable as non-aqueous solvents that permit desirable reactions to occur for drug delivery purposes. Gel drying with supercritical CO_2 leads to structures most similar to the extracellular matrix, even when the chitosan is crosslinked, or in combination with metal oxides of interest in orthopedics.

Keywords: chitin; chitosan; electrospinning; ionic liquids; nanofibrils; supercritical carbon dioxide

1. Introduction

A large body of knowledge exists today on the use of chitosans as safe biomaterials for a variety of applications: there are recent review articles in biomedical sciences [1–6] and in pharmaceutical sciences [7–15]. Besides the review articles most directly dealing with chemical approaches [16–21], some are focused on the preparation and applications of carboxymethyl and succinyl derivatives of

chitin and chitosan with particular attention to their biomedical applications [22]; on the hydrophobic modifications of chitosans mainly for gene delivery in comparison with polyethyleneimine and polylysine [23], while more general treatments are also available [24–26]. Reviews on the safety of chitin have been published recently [27,28].

Chitins and chitosans and their beneficial characteristic properties could certainly be even further improved by more elaborate refinements of the technological approaches to enable further exploitation of the amply available chitin resources. The scope of the present review article is to provide technical details and evaluations of results, suitable for the appreciation of the immediate potential developments of the title technologies.

2. Chitin and Chitosan Nanofibrils

In the area of the isolation and characterization of nanofibrils (otherwise called chitin nanocrystals, or whiskers), significant scientific and technological advances have recently been made. In particular, articles were published dealing with: (i) disassembly of chitin for the isolation of nanochitin by mechanical means in the presence of minor amounts of acetic acid; (ii) disassembly of chitosan; (iii) preparation of nanochitosan from partially deacetylated chitin.

2.1. Mechanical Disassembly of Chitin Nanofibrils

Chitin nanofibers were prepared by Kose and Kondo [29] by using the aqueous counter collision method that provided homogeneous aqueous dispersion of chitin nanofibers having a width of 10–20 nm. The mechanical disassembly of chitin has suddenly attracted much attention: in fact, suspensions of crude α-chitin were treated first with a blender, and then the slurry of 1% purified chitin was passed through a grinder at 1500 rpm, with a clearance gauge of 0.15 mm shift as demonstrated by Ifuku *et al.* [30].

The same team developed the concept that it would be advantageous to enhance the cationic repulsion existing between chitin fibers with the aid of partial protonation in order to disassemble the chitin: a protonation degree as small as 4% or less is sufficient to weaken the hydrogen bonds that protect the tight chitin structure [31]. Various industrial chitins, including the α-polymorphs, by this route yield nanofibrils having a high degree of crystallinity and 10–20 nm cross-section.

According to Shams *et al.* [32] several drops of acetic acid were added to the 1% slurry of purified wet chitin to adjust the pH value at 3–4 and to facilitate the fibrillation: the suspension was then blended for 10 min at a speed of 37,000 rpm, and kept in a never-dried condition. The neutralized disassembled nanofibrils were dispersed in water (0.1%) and a colloidal structure was obtained, indicating that the chitin fibrils were homogeneously dispersed: it was vacuum-filtered on a polytetrafluoroethylene membrane (0.1 μm porosity) to produce a dry sheet having diameter 9 cm, thickness 55 μm, and density 1.0 g/cm^3. The dried sheets were impregnated with neat acrylic resin (refractive index 1.536) in such a way as to obtain transparent nanocomposites, with 40% chitin content. The width distribution evaluated directly from the SEM images demonstrated that almost 70% of the nanofibril width was in the range 20–30 nm. The degree of *N*-acetylation 0.93 of the nanofibers was obtained by elemental analysis and indicated that no deacetylation occurred in the course of the treatment. Furthermore, the polysaccharide did not lose its transparency because fibers or

particles which have such a small diameter do not produce light scattering; as a consequence it was claimed useful for optical devices. As an extension of that work, optically transparent chitin nanofibril composites were fabricated with 11 different types of (meth)acrylic resins. Chitin nanofibers significantly increased the Young's modulus and the tensile strength, and decreased the thermal expansion of all (meth)acrylic resins due to the reinforcement effect of chitin nanofibers endowed with extended crystal structure [33,34].

Incidentally, under the same conditions, ultrasonication was applied to the chitin slurries for 2 min using an ultrasonic homogenizer at 19.5 kHz and the 300 W output power (probe tip diameter 7 mm); the temperature increase was <5 °C during the ultrasonication [35].

The disadvantages of the earlier preparation methods were numerous and included low yield, dangerous handling of boiling HCl, disposal of the colored HCl solution, recovery of enormous quantities of slightly acidic water, difficult adjustment of the pH value because of the strength of HCl, scaling-up troubles and excessive costs. The new technology that permits today the treatment of industrial chitin dry powders instead of "never dried" chitins removes the most important limitation of the large-scale production of nanochitin. This technology provides a significant advantage towards chitin exploitation, in terms of transportation costs, stable supply, shelf life and storage space, since chitin nanofibers can be prepared from light, low volume, and non-perishable dry chitin.

2.2. Mechanical Disassembly of Chitosan Nanofibrils

High-pressure homogenization was combined with wet-grinding to disassemble suspended chitosan particles into nano-chitosan [36]. The chitosan slurry was forced to pass through the wet-grinding machine at the flow rate of 10 L/h and then it was poured into the stainless-steel tank of a Microfluidizer (M-100P, Microfluidics Corp. MA, USA) equipped with a pair of ceramic (200 μm) and diamond (87 μm) interaction chambers; it was cooled and then released back to the tank for the next cycle. Under the pressure of 207 MPa, the ground slurry passed 10 times through the interaction chambers at the flow rate of 8 L/h; then, the homogenized chitosan slurry was centrifuged at 1000 rpm for 5 min to remove the sediment and to yield a homogeneous chitosan suspension that was used to prepare a high strength liquid crystal thin film at relatively low temperature. There was no pattern or fingerprint found in the control cast films, meaning that chitosan nanofibrils self-assembled with cholesteric structure. Whilst the chitosan cast film possessed high tensile strength (about 35.8 ± 7.6 MPa) and Young's modulus (about 580.0 ± 21.8 MPa), the chitosan liquid crystal film had higher values up to 100.5 ± 4.0 MPa, and 2.2 ± 0.2 GPa, respectively, that are typical for liquid crystalline polymers [37].

2.3. Nanochitosan Obtained from Partially Deacetylated Chitin, or from Deacetylated Nanochitin

For this preparation, the deacetylation of chitin nanofibrils was made with 50% NaOH in the presence of borohydride; the molecular weight dropped to 59 kDa, much lower than the one of chitosan from chitin powder under the same conditions (422 kDa) [38]. The degree of deacetylation was 0.50 and the suspensions were colloidal at 1–13%. The new methods however opened new routes directly to nanofibrillar chitosan, which is more versatile than chitin. The fine chitin powder was also deacetylated in a relatively mild way, thus producing nano-chitosan that underwent homogeneous dispersion at pH 3–4 [39].

2.4. Applications

From the cell walls of five different types of mushrooms, chitin nanofibrils were isolated by removing glucans, minerals, and proteins, and subsequent grinding treatment under acidic conditions as described above. The chitin nanofibrils thus obtained by Ifuku *et al.* [40] were characterized by elemental analysis, FTIR spectrometry, and X-ray diffraction; they had uniform structure and were unusually long. The width of the nanofibers was in the range 20–28 nm and depended on the type of mushroom. The results showed that the α-chitin structure was maintained and glucans remained on the nanofiber surface. It was deemed that the said nanofibrils of fungal origin might have anti-tumor applications and immune-modulating activity.

Exhaustive studies were made by Muzzarelli *et al.* [41] who incorporated crustacean chitin nanofibrils into wound dressings made of chitosan glycolate and dibutyryl chitin that were applied in a variety of traumatic wounds with limited number of changes and excellent final healing; the nanofibrils were characterized with advanced instrumental analytical techniques (Figure 1).

Figure 1. FTIR spectrum of spray-dried α-chitin nanofibrils ready for incorporation in a chitin + chitosan composite used for wound dressing. This spectrum showed for the first time unmatched resolution of all typical chitin bands. Reprinted from [41]. Copyright (2007) with permission from Elsevier.

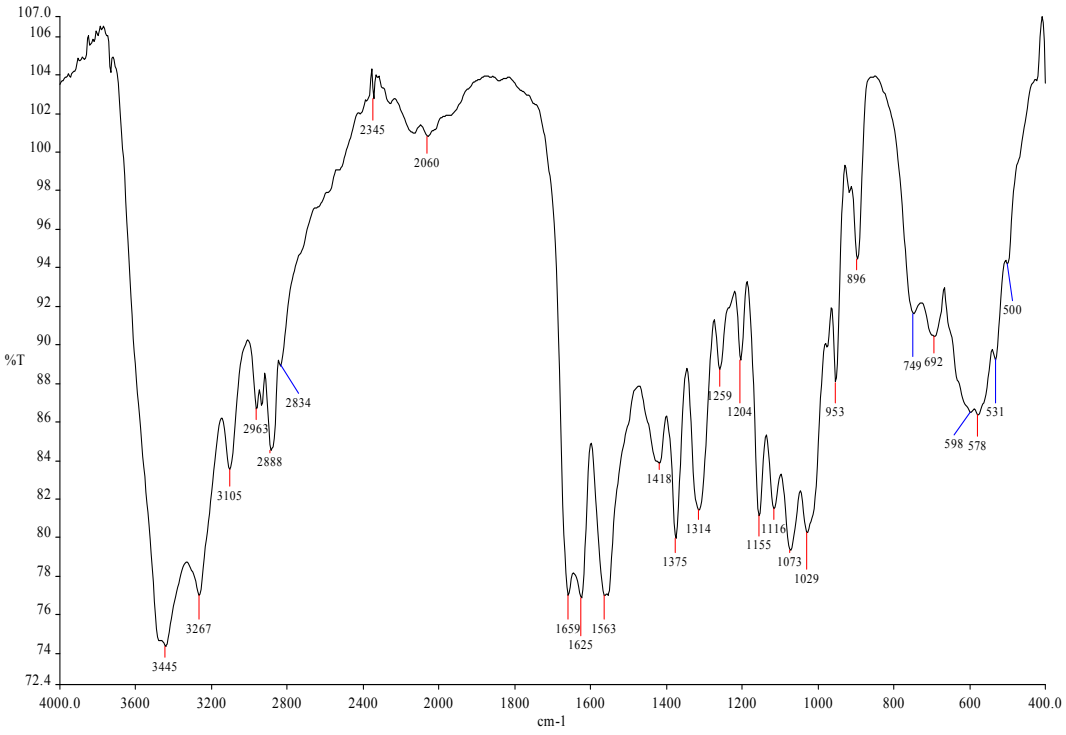

Han *et al.* [42] investigated the influence of chitosan nanofiber scaffold on the production and infectivity of porcine endogenous retrovirus expressed by porcine hepatocytes. Freshly isolated porcine hepatocytes were cultured with a chitosan nanofiber scaffold, that prolonged the porcine endogenous retrovirus secreting time in pig hepatocytes, but did not appreciably influence its productive amount and infectivity, so it could be applied in the bioartificial liver without risk of virus transmission.

Chitin nanofibrils 5–10 nm diameter were employed by Ma *et al.* [43] as barrier layers in a new class of thin-film nanofibrous composite membranes for water purification. The very high surface-to-volume ratio leads to high virus adsorption capacity as verified by MS2 bacteriophage testing, and offers further opportunities in drinking water applications. The low cost of raw chitin, the environmentally friendly fabrication process, and the impressive high flux indicate that such ultrafine nanofibril-based membranes can surpass conventional-membranes in many water applications.

The chitin nanofibrils were effective in stabilizing oil-in-water emulsions against coalescence, presumably because of the adsorption of the nanofibrils at the oil–water interface. The rheological data provided evidence for network formation in the emulsions with increasing chitin nanocrystal concentration. Such a gel-like behavior was attributed to the formation of a chitin nanocrystal network in the continuous phase. The stability of the emulsions to creaming increased linearly with nanofibril concentration [44].

Several more applications of chitin nanofibrils have already been developed, for example, waterborne polyurethane-based nanocomposites were prepared by Huang *et al.* [45] by incorporating small quantities of chitin nanofibrils as the nanophase: the nanofibrils loading of 3% showed the maximum tensile strength (28.8 MPa) and enhanced the Young's modulus (6.5 MPa), ~1.8- and 2.2-fold over those of neat polyurethane. The active surface and rigidity of nanofibrils facilitated formation of the interface for stress transferring and provided endurance to stress. The incorporation of chitosan nanofibrils in alginate fibers was achieved by mixing homogenized chitosan nanofibrils colloidal suspension with 6% w/v sodium alginate aqueous solution, followed by wet spinning [38].

Porous bone scaffolds with enhanced physical, mechanical and biological performances were prepared with hyaluronan and gelatin (1:1 w/w blend), and the reinforcing filler was α-nanochitin; 1-ethyl-3-(3-dimethylaminopropyl) carbodiimide was used as a crosslinker [46]. The weight ratios of the nanochitin to the blend were up to 30%, the average pore size of the scaffolds ranged between 139 and 166 μm, regardless of the nanochitin content, but the incorporation of 2% nanochitin in the scaffolds doubled their tensile strength. The as-prepared nanochitin was in the form of slender rods with sharp ends (255 ± 56 × 31 ± 6 nm, with L/d aspect ratio ~8). Although the addition of 20–30% nanochitin improved thermal stability and resistance to biodegradation, the scaffolds with 10% were the best for supporting the proliferation of cultured human osteosarcoma cells.

Melatonin was adsorbed on the nanofibrils [47,48]; lipoic acid was likewise treated [49]. Glycerol plasticized-potato starch was mixed with chitin nanofibrils to prepare fully natural nano-composites by casting and evaporation: this led to improvements in tensile strength, storage modulus, glass transition temperature, and water vapor barrier properties of the composite. However, at >5% loading, aggregation of the nanofibrils took place with negative effects [50]. On the other hand, the effect of different concentrations of cellulose nanofibers, and plasticizer (glycerol) on tensile properties, water vapor permeability, and glass transition temperature of chitosan edible films were evaluated to work out a formulation that optimized their properties: the nanocomposite film with 15% cellulose nanofibers and 18% glycerol, comparable to some synthetic polymers in terms of strength and stiffness [51].

Chitin nanofibrils were acetylated to modify the fiber surface: the acetylation degree could be controlled from 0.99 to 2.96 by changing the reaction time. After a short acetylation (1 min), the moisture content of the nanocomposite decreased from 4.0 to 2.2%. The nanofibril shape was maintained and the thickness of the nanofibrils increased linearly with the acetylation degree.

Composites containing the acetylated chitin nanofibrils (25%) in acrylic resin were fabricated [34]. Nanofibers based on poly(vinyl alcohol) as the matrix, and α-chitin nanofibrils (~31 nm × ~549 nm) were prepared [52]. Chitin nanofibrils were blended with polylactide to form organic composites, and with apatite or rectorite to form inorganic composites suitable for food-packaging applications [53–55].

3. Electrospun Nanofibers

Electrospun natural biopolymers are of great interest in the field of regenerative medicine due to their unique structure, biocompatibility, and potential to support controlled release of bioactive agents and/or the growth of cells near a site of interest. However, the scaling-up of chitosan nanofiber fabrication by electrospinning is problematic and challenging. First of all, solutions with a high concentration of chitosan are not injectable, while those with a very low concentration result in a low output rate. On the other hand, the large quantity of organic solvents used during the electrospinning process alters/denatures the structure and properties of the natural chitosan. Furthermore, due to its polyelectrolyte nature, chitosan cannot be continuously spun as droplets persistently form. It is well known that pore size and structure of a scaffold play a vital role in cell cultures because they are responsible not only for the adhesion, migration, and distribution of cells, but also for the exchange of nutrients and metabolic waste. Despite numerous efforts, issues relating to mechanical strength, uniformity, interconnections and porosity of nanofiber mats have not yet been solved.

3.1. Chitosan + Nylon Electrospun Nanofibers

The electrospun chitosan has been characterized by Nirmala *et al.* [56] with the aid of the most advanced analytical instrumentation: they found that the chitosan nanofibers had diameters ranging from 10 to 1200 nm, and anisotropic nature. Their stability was studied by Cooper *et al.* [57], while Jacobs *et al.* [58] optimized the electrospinning parameters for chitosan nanofibers.

Electrospinning offers unique possibilities when a single compound dissolves both chitosan and an artificial polymer, this being the case for chitosan and nylon, so that the biochemical properties of chitosan can be associated to the mechanical properties of nylon: outstanding performances can be expected from such a composite, as mentioned by Muzzarelli [59] for the recovery of metals from sea-water. A work by Nirmala *et al.* [60] focused on the preparation of chitosan blended polyamide-6 nanofibers by a single solvent via electrospinning, to be used for cultures of human osteoblasts. The nanofibers were well oriented and had good incorporation of chitosan. Infrared spectrometry indicated that the amino groups of chitosan still existed in the blended nanofibers. The morphological features of the cells attached to nanofibers were observed by SEM. The adhesion, viability and proliferation properties of osteoblast cells on the polyamide-6 + chitosan blended nanofibers were analyzed by *in vitro* cell compatibility test. In a further work, Nirmala *et al.* [61] reported that current-voltage measurements revealed interesting linear relation, including enhanced conductivity with respect to chitosan content. The electrical conductivity of the polyamide-6 + chitosan composite nanofibers increased with increasing content of chitosan due to the formation of ultrafine nanofibers. In addition, the sheet resistance of composite nanofibers decreased with increasing chitosan concentration.

A totally different approach was followed by Zhang *et al.* [62]: electrospun nylon-6 nanofibrous membrane with fiber diameters in the range of 50–200 nm were prepared and employed as affinity

material for papain adsorption due to their excellent chemical and thermal resistance as well as high wettability. Covalent coupling of chitosan to activated nylon membrane was performed after the reaction of the nanofibrous nylon membrane with formaldehyde. The dye Cibacron Blue F3GA as a ligand was then covalently immobilized on the chitosan-coated membranes, to be used for papain collection, with adsorption capacity up to 133.2 mg/g.

3.2. Applications in Cardiology

Hussain *et al.* [63] explored electrospun chitosan-based nanofiber scaffolds for cardiac tissue engineering. In the 2D and 3D scaffolds, only the cardiomyocyte-fibroblasts co-cultures resulted in polarized cardiomyocyte morphology, and the expression of sarcomeric actin and connexin-43 was higher than under other culture conditions. Said fibroblasts co-cultures demonstrated synchronized contractions involving large tissue-like cellular networks. This was the first attempt to utilize 3D chitosan nanofibers as cardiomyocyte scaffolds with the result that cardiomyocyte retained their morphology and function. Other applications in cardiology were proposed by Cynthia *et al.* [64] who tested mechanical properties, biocompatibility and cell retention ability of gelatin-chitosan polyurethane. In fact, for a proper function of the cardiac valve the materials selected for the leaflets need to be biocompatible, robust, flexible, and have comparable mechanical properties to the natural ones. Native heart valve leaflets are subjected to continuous pulsatile and homodynamic forces and can be as thin as 300 μm. Endothelial cells, isolated from ovine carotid arteries were seeded onto these materials and exposed to a range of shear-stresses for a period of 1–3 h. Throughout the exposure time and the shear stress values tested, a mean cell retention of 80% was obtained in the gelatin-chitosan polyurethane group. Noticeably for the full range of physiological flow conditions tested, the electrospun gelatin-chitosan polyurethane demonstrated good biocompatibility and cell retention properties.

Likewise, scaffolds for blood vessel and nerve conduits, were designed on the basis of collagen-chitosan-thermoplastic polyurethane electrospun to mimic the components and the structural aspects of the native extracellular matrix. The scaffolds were crosslinked with glutaraldehyde vapor to prevent them from being dissolved in the culture medium. Cell viability studies with endothelial cells and Schwann cells demonstrated that the electrospun composite nanofibrous scaffolds had good biocompatibility, and that the aligned fibers could regulate cell morphology by inducing cell orientation. Vascular grafts and nerve conduits were electrospun or sutured based on the nanofibrous scaffolds: the results indicated that collagen-chitosan-polyurethane blended nanofibrous scaffolds might be suitable for vascular repair and nerve regeneration [45].

3.3. Other Preparations of Biomedical Interest

An alternative to the experiments described above is the esterification of chitosan with the use of lactide or polylactide: both chitosan and polylactide/polyglycolide have good biocompatibility and can be used to produce scaffolds for cultured cells. However the synthetic scaffolds lack groups that would facilitate their modification, whereas chitosan has extensive active amine and hydroxyl groups which would allow subsequent modification intended for the attachment of peptides, proteins and drugs. Moreover chitosan is very hydrophilic, whereas poly(D,L-lactide-co-glycolide) (PLGA) is relatively hydrophobic. Accordingly there are many situations where it would be ideal to have a copolymer of

both, especially one that could be electrospun to provide a versatile range of scaffolds for tissue engineering. In a study by Xie *et al.* [65], chitosan was first modified with trimethylsilyl chloride, in the presence of dimethylamino pyridine. PLGA-grafted chitosan copolymers were prepared by reaction with end-carboxyl PLGA (PLGA-COOH). Elemental analysis showed segments with an average of 18-pyranose units when PLGA-COOH was grafted into the chitosan chain. Contact angle measurements demonstrated that copolymers became more hydrophilic than PLGA. The chitosan-g-PLGA copolymers were electrospun to produce either nano- or microfibers as desired. A 3D fibrous scaffold of the copolymers gave good fibroblast adhesion and proliferation which did not differ significantly from the performance of the cells on the chitosan or PLGA electrospun scaffolds.

Chitosan derivatives were prepared by Skotak *et al.* [66] following a "one pot" approach by grafting L-lactide oligomers. Chitosan was dissolved in methanesulfonic acid, followed by the addition of the L-lactide monomer. This reaction mixture was stirred for 4 h at 40 °C under an argon atmosphere. The side chain had values between 4.6 and 14 units. On average, there were two side chains of oligo-L-lactide per glucosamine ring, and their length depended on the initial reagents ratio. L-Lactide grafted chitosan samples display cytotoxicity over a range of substitution degree values, as demonstrated with fibroblast cultures. This synthetic route renders the esterified chitosans soluble in a broad range of organic solvents, facilitating formation of ultrafine fibers via electrospinning.

Likewise, from blended solutions of chitosan and poly(ethylene oxide) (PEO), chitosan-based defect-free nanofibers with average diameters from 62 ± 9 nm to 129 ± 16 nm were fabricated [67]. The use of polysorbate surfactant Tween 20 to improve the functionality of the nanofibers was studied by Ziani *et al.* [68] with two highly deacetylated chitosans (MW 148 and 68 kDa) dissolved with acetic acid and then mixed with PEO. Because pure chitosan dissolved in different acid concentrations did not form fibers but beads, addition of PEO was necessary to electrospin the chitosan solutions. Average fiber diameters and size distribution depended on acidity and molecular weight. Solutions of chitosan + PEO + surfactant were effectively electrospun. The presence of surfactant resulted in decrease of surface tension and in the formation of smooth fibers.

Cationic nanofibrous mats are expected to show improved cellular adhesion and stability. Caprolactone oligomers were grafted onto the hydroxyl groups of chitosan via ring-opening polymerization by using methanesulfonic acid as solvent and catalyst: then, nanofibrous mats were obtained by electrospinning. The content of amino groups on the nanofiber surface increased linearly with the quantity of grafted chitosan, as revealed by the increased zeta-potential of nanofibers. Chitosan-*g*-oligo(caprolactone) in poly(caprolactone) (2/8) mats with moderate surface zeta-potential (3 mV) were the best in promoting mouse fibroblast attachment and proliferation. Toluidine blue staining confirmed that said cells grew well and exhibited a normal morphology [69]. Chitosan/poly(caprolactone) nanofibrous scaffold was prepared in a single step by Shalumon *et al.* [70]. The presence of chitosan in the scaffold imparted improved hydrophilicity to the scaffold, as confirmed by decreased contact angle, which thereby enhanced bioactivity and protein adsorption on the scaffold, which was found to be cyto-compatible.

Feng *et al.* [71] developed a method to obtain high surface area nanofiber meshes composed of chitosan of various molecular weights. These chitosan nanofiber meshes were developed as a culture substrate for hepatocytes: they exhibited a uniform diameter distribution (average 112 nm) and

stability. The chitosan nanofibers were biocompatible with hepatocytes and were expected to be useful for artificial liver and for liver regeneration.

Aligned and randomly oriented poly(D,L-lactide-co-glycolide) + chitosan nanofibrous scaffolds have been prepared by electrospinning [72]. The release of the drug fenbufen from the fenbufen-loaded aligned and randomly oriented PLGA and PLGA/chitosan nanofibrous scaffolds increased with the increase of chitosan content. Moreover, the nanofiber arrangement influenced the release behavior. Crosslinking in glutaraldehyde vapor contributed to decrease the burst release of the drug from the loaded PLGA/chitosan nanofibrous scaffold.

Gelatin and chitosan nanofibers were electrospun and then cross-linked by glutaraldehyde vapor at room temperature. The cross-linked mats kept their nanofibrous structure after being soaked in deionized water at 37 °C. The two main chemical reactions of cross-linking for chitosan and gelatin-chitosan complex are Schiff base reaction and acetalization. The mechanical properties of nanofibrous mats were improved after cross-linking. The biocompatibility of electrospun nanofibrous mats after cross-linking was investigated by the viability of porcine iliac endothelial cells [73].

Silk fibroin + hydroxybutyl chitosan nanofibrous scaffolds were fabricated by electrospinning by using hexafluoro-2-propanol and trifluoroacetic acid as solvents to mimic the extra-cellular matrix. Both tensile strength and elongation at break were remarkably improved when the weight ratio of fibroin to hydroxybutyl chitosan was 20:80. The use of genipin vapor not only induced conformation of fibroin to convert from random coil to beta-sheet structure but also acted as a cross-linking agent for fibroin + hydroxybutyl chitosan [74].

As an example of versatility of the chitosan derivatives, a new method was presented by Almodovar and Kipper [75] for functionalizing electrospun nanofibers with GAGs and growth factors by polyelectrolyte multilayers deposition. Chitosan nanofibers, electrospun from trifluoroacetic acid and dichloromethane, were coated with heparin and N,N,N-trimethyl chitosan. FGF-2 was adsorbed on the PEM-coated nanofibers.

Electrospun nanofibers can be mineralized. The chitosan/poly(vinyl alcohol) nanofibers produced thin $CaCO_3$ crystals that interlaced with the chitosan fiber not only on the surface of the membrane but also within it. The crystals developed into a continuous $CaCO_3$ membrane on the fibers at a late stage of mineralization: the crystals were mainly calcite with a small quantity of vaterite. The attachment and growth of mouse fibroblast occurred evenly on the surface of the mineralized composite membrane [76].

Espindola-Gonzalez *et al.* [77] studied structural and thermal properties of chitosan + starch + poly(ethylene terephthalate) (PET) fibers manufactured via electrospinning. Addition of PET to chitosan + starch systems resulted in improved thermal stability at elevated temperatures.

Kim and Lee [78] reported that the combination of electrospraying and subsequent freeze-drying can produce chitosan fibrous 3D network structures from low concentration chitosan solutions, well below fiber forming concentrations. Nanoparticle suspensions of chitosan were first fabricated by a controlled electrospraying process, and then the freeze-drying process promoted the assembly of the nanoparticles into fibrous networks. Figure 2 shows the typical fibrous structures obtained by electrospraying and subsequent freeze drying: the average diameter of a strand was 0.5–3 μm and the surface area of the fibers was 17.8 ± 0.39 m^2/g. The nanofibrils, showing interconnections with each other were exempt from the bead-string motifs often found in electrospun fibers. The surface of these

nanofibrils is different from those of conventional fibers insofar as it has no significant textures resulting from stretching processes, as a point of difference from the surface of most chitosan fibers.

Figure 2. SEM micrograph of chitosan nonwoven fabrics obtained by electrospraying and subsequent freeze drying. Reprinted from [78]. Copyright (2011) with permission from Elsevier.

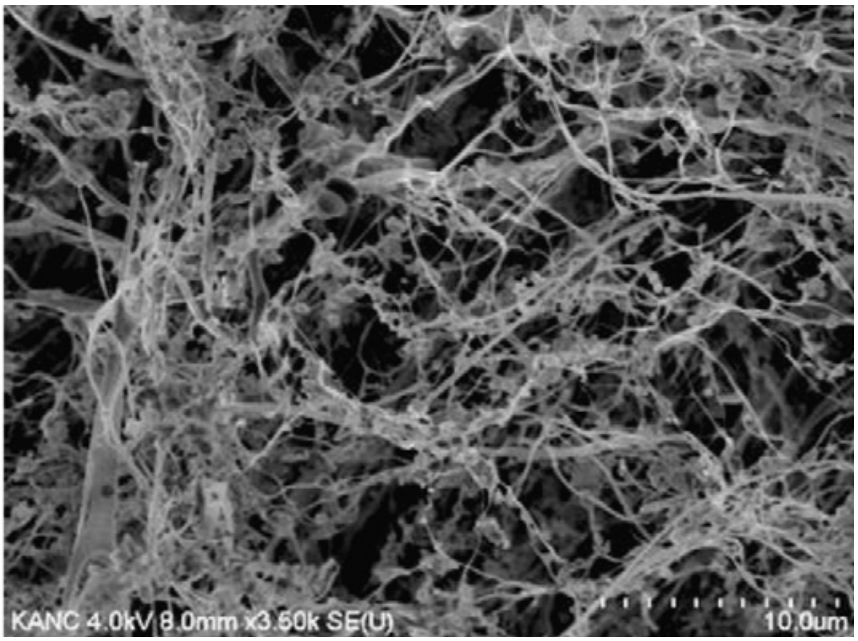

Chitosan, sodium chondroitin sulfate, and pectin-nanofibrous mats were prepared from the respective polysaccharide/poly(ethylene oxide) blend solutions by electrospray. Unblended polysaccharide solutions showed low processability; viz., the solutions could not be electrosprayed. The addition of 500 kDa poly(ethylene oxide) to chitosan solutions enhanced the formation of a fibrous structure. Sodium chondroitin sulfate/poly(ethylene oxide) and pectin/poly(ethylene oxide) blend solutions were generally too viscous to be sprayed at 25 °C, but at 70 °C the fibrous structure was formed [79].

Chitosan fibers showing narrow diameter distribution with a mean of 42 nm were produced by electrospinning and utilized for the sorption of Fe(III), Cu(II), Ag(I), and Cd(II) ions from aqueous solutions. By virtue of its mechanical integrity, the applicability of the chitosan mat in solid phase extraction under continuous flow looks interesting: the surface area calculated from the isotherms to be about 0.92 m^2/g for the powder and 22.4 m^2/g for the electrospun fibers, indicates that electrospinning introduced a 20-fold increase of the surface area of chitosan [80]. Of course this kind of data on the chelating capacity of nanofibrous mats endowed with large surface area can be extended to the enhancement of the antibacterial activity of silver chelates of this kind. In fact, electrospun chitosan + poly(vinyl alcohol) nanofibers functionalized with silver nanoparticles had 220–650 nm diameter, and the silver nanoparticles embedded into the fibers exerted high antibacterial activity against *E. coli* [81]. Data assessing the doping effects of monovalent, bivalent and trivalent metal ions on the morphological appearance of the electrospun chitosan + poly(ethylene oxide) blend nanofibers were made available by Su *et al.* [82].

Chitosan nano-powders were modified using hydrazine plasma produced at low pressure (26.66 Pa) with 13.56 MHz frequency at 100 W for 30 min. Chitosan and plasma-modified chitosan in poly(vinyl alcohol) (PVA) solutions were used to produce nanofibers by electrospinning, with average fiber diameters 480 and 280 nm, respectively. The antibacterial effect of the treated chitosan was enhanced [83]. The spinnability of chitosan with PVA was optimized by Huang *et al.* [84].

4. Ionic Liquids: New Reaction Media

The ionic liquids have emerged as a class of organic salts that can be used as components of polymeric matrices, templates for porous polymers and solvents for a wide variety of organic and inorganic compounds. They are liquids at room temperature and exhibit unique physico-chemical properties, namely no vapor pressure, excellent chemical and thermal stability, high ionic conductivity and easy recyclability. Their use as solvents or non-volatile reaction media instead of conventional organic solvents can minimize a number of environmental and safety problems. They have provided a new processing platform for the dissolution of cellulose, chitin, starch and lignin: the macromolecules can be dissolved, regenerated and functionalized, thus increasing their chances of exploitation.

Not so much information on the dissolution of chitin in ionic liquids is present in the literature yet, because attention was immediately captured by cellulose that is dissolved likewise: typical ionic liquids in this context are 1-allyl-3-methylimidazolium chloride (AmiCl); 1-butyl-3-methylimidazolium chloride (BmiCl), and 1-butyl-3-methylimidazolium acetate (BmiAc) [85].

Xie *et al.* [86] used BmiCl and declared that up to 10% of chitin could be dissolved within 5 h at 110 °C; however, this finding was questioned because results were not reciprocally comparable, presumably due to the diversity of chitin in terms of polymorphic form, different origin, molecular weight and degree of acetylation.

An acidic cellulose + chitin gel electrolyte made of cellulose, chitin, 1-butyl-3-methylimidazolium, 1-allyl-3-methylimidazolium bromide, and an aqueous H_2SO_4 solution was investigated for electric double layer capacitors with activated carbon fiber cloth electrodes. The acidic cellulose + chitin hybrid gel electrolyte has practical applicability to an advanced electric double-layer capacitor with excellent stability and working performance [87]. Rheological evaluations on the clear solution of 5% chitin in 1-allyl-3-methylimidazolium bromide (obtained at 100 °C for 48 h) showed that it behaved like weak gels [88]. Chitosan + cellulose composite fibers from an ionic liquid medium were obtained by electrospinning [89].

Another example was provided by Takegawa *et al.* [90] who prepared chitin + cellulose composite gels and films using the two ionic liquids, 1-allyl-3-methylimidazolium bromide and 1-butyl-3-methylimidazolium chloride. Both polysaccharides were dissolved separately and then the two liquids were mixed in various ratios at 100 °C to give homogeneous mixtures: gels were obtained after 4 days. Moreover, films made of chitin + cellulose were obtained by casting the mixtures on glass plates, followed by soaking in water and drying: the obtained gels and films were characterized by X-ray diffraction spectrometry and thermo-gravimetric analysis. The mechanical properties of the gels and films were evaluated under compressive and tensile modes, respectively [90]. More data by Wu *et al.* [91] and by Kadokawa *et al.* [92] relevant to the solubility of chitins and chitosans in said ionic liquids are collected in Table 1.

Table 1. Solubility of isolated chitins and chitosan in 4 ionic liquids. Based on data in [91,92].

Polymer	Origin and viscosity	Solubility (w/w%) at 110 °C			
		AmiCl	**AmiBr**	**BmiAc**	**BmiCl**
α-Chitin	Crab	n.a.	Soluble, 9.1	n.a	n.a.
α-Chitin	Crab, η 35 cp	Insoluble	n.a.	Soluble, 6	Partly soluble
β-Chitin	Squid pen, η 15 cp	Insoluble	n.a.	Soluble, 7	Partly soluble
β-Chitin	Squid pen, η 278 cp	Insoluble	n.a.	Soluble, 3	Insoluble
Chitosan	Crab, Mv 97 kDa	Soluble, 8	n.a.	Soluble, 12	Soluble, 10

AmiCl is 1-allyl-3-methylimidazolium chloride; BmiCl is 1-butyl-3-methylimidazolium chloride, BmiAc is 1-butyl-3-methylimidazolium acetate, and AmiBr is 1-allyl-3-methylimidazolium bromide. n.a. = not available.

The dissolution behavior of chitin in a series of ionic liquids containing alkylimidazolium chloride, alkylimidazolium dimethyl phosphate, and 1-allyl-3-methyl-imidazolium acetate has been studied by Wang *et al.* [93]. The dissolution behavior of chitin in ionic liquids was affected by the degree of acetylation, the degree of crystallinity, and the molecular weight of chitin, as well as by the nature of the anion of the ionic liquid. Moreover, 1-ethyl-3-methyl-imidazolium acetate dissolves raw crustacean shells completely, leading to the recovery of highly pure chitin of high molecular weight, in the form of powder, films and fibers directly spinnable from the extract solution [94].

Polyacrylamide was used by Zhou and Wu [95] as a matrix material for fabricating novel nanocomposite hydrogels reinforced with natural chitosan nanofibers via *in situ* free-radical polymerization. The chitosan nanofibers established hydrogen and covalent bonds with polyacrylamide, and acted as a multifunctional cross-linker and a reinforcing agent in the hydrogel system. The compression strength and storage modulus of the nanocomposite hydrogels were significantly higher than those of the pure polyacrylamide hydrogels. The 1.5% chitosan nanofibers loading showed the best combined swelling and mechanical properties of the hydrogels.

Chitin nanofibrils were easily formed by the gelation of commercial chitin powders with 1-allyl-3-methylimidazolium bromide followed by the regeneration with methanol, according to Kadokawa *et al.* [92]. By using poly(vinyl alcohol) prior to methanol, nanofibrils ~20–60 nm in width and several hundred nanometers in length were obtained. The key point of this facile preparation is that chitin was swollen with said ionic liquid at room temperature, followed by heating at 100 °C (Table 1). Then, a solution of PVA (1.25 mmol, 0.0750 g) in hot water (3.0 mL) was mixed to the gel at 80 °C with stirring; methanol (40 mL) was slowly added to the resulting mixture, and the system was left standing at room temperature for 24 h, followed by sonication to give a dispersion of chitin nanofibrils. Filtration of the dispersion was carried out to give a chitin film.

Hua D.B. *et al.* [96] reported the conjugation of hydrophobic drugs with chitosan, via Schiff reaction in an ionic liquid, which renders chitosan soluble in common organic solvents and amenable to further functional modifications. For example, thermo-responsive poly(*N*-isopropylacrylamide) was grafted to the chitosan-drug conjugate. The graft copolymer self-assembled in water at neutral pH into core-shell nanocarriers with size distribution ~142 ± 60 nm, favorable for intravenous administration. At 37 °C and pH 4.5 (conditions mimicking endosomal or lysosomal uptake) the nanocarriers formed reversed micelles (~8 ± 3 nm) favoring clearance by renal filtration, and 70% of the drug was liberated within 30 h through hydrolytic cleavage of the Schiff base conjugation. Based on the smart drug

release profile said approach was deemed viable for the intravenous administration of hydrophobic drugs carried by chitosan-based vehicles.

1-Butyl-3-methyl-imidazolium chloride was used for auto-templating assembly of $CaCO_3$ and chitosan to produce well-defined hollow inorganic-organic nanoboxes and nanoframes. By varying the experimental conditions, size and shell-thickness of hollow nanostructures were adjusted in the ranges 200–400 nm and 15–75 nm, respectively [97].

The hybrid film of gold nanoparticles + ionic liquid + chitosan was used as an efficient immobilization matrix to fabricate an immunosensor. The film produced a well-defined voltammetric signal due to the synergistic effects of the ionic liquid and gold nanoparticles. By immobilizing an alkaline phosphatase-labeled antibody in said film, a sensitive amperometric immunosensor was developed for the prostate specific antigen (PSA). Under the optimized conditions, the immunosensor exhibited a linear range from 1.0 to 80 ng/mL of PSA [98]. In a similar fashion, Safavi *et al.* [99] prepared biosensors based on the electrocatalysed reduction or hydrogen peroxide at the electrode coated with cholesterol oxidase. The biosensor exhibited two wide linear ranges of response to cholesterol for concentrations of 0.05–6.2 and 6.2–11.2 mM. The sensitivity was 90.7 $\mu A \cdot mM^{-1} \cdot cm^{-2}$, the limit of detection was 101 μM of cholesterol, and the response time was <7 s.

Porous chitin-based materials were developed by Silva *et al.* [100] who combined the processing of chitin using ionic liquids together with the use of supercritical fluid technique, to provide a clean technology. Chitin was dissolved in 1-butyl-3-imidazolium acetate, followed by regeneration of the polymer in ethanol in specific moulds. The ionic liquid was removed using Soxhlet extraction and successive steps of extraction with supercritical fluid process using carbon dioxide/ethanol ratios of 50/50 and 70/30. Ultralight porous chitin structures were produced while the efficiency of the ionic liquid removal was measured by conductivity. The developed chitin matrices showed interesting features, such as: (i) low crystallinity resulting from loose hydrogen bonds in the chitin structure; (ii) wide mesoporous distribution; (iii) very low density (0.039–0.063 g/L); (iv) porosity between 84 and 90%, and (v) extremely low cytotoxicity for L929 fibroblasts.

5. Supercritical Drying

The popularity of supercritical carbon dioxide(sc-CO_2) stems from the fact that it is nontoxic, nonflammable, promptly available in large amounts, and that it is the second least expensive solvent after water. A special issue devoted to sc-CO_2 has been published in 2011 by the Journal of Supercritical Fluids. An interesting property associated with the critical state is that the density of the liquid and of the vapor becomes identical, and for this reason the interface between them disappears. Supercritical carbon dioxide is most widely used thanks to its easily accessible critical temperature and pressure (31.2 °C; 7.4 MPa). Supercritical fluid technology is a relatively new technique to obtain micro- and nano-particles: many drugs can be dissolved or liquefied in sc-CO_2 before being sprayed through a nozzle upon depressurization to produce fine drug particles. It is possible to take advantage from high supersaturation of drugs in sc-CO_2, which contributes to the particle size reduction; as an alternative, sc-CO_2 can be used as an antisolvent for the precipitation of drugs from organic solutions [101]. For polar and high MW polymers, the sc-CO_2 solvent power is unfortunately low, and the use of amphiphiles might be necessary: surfactants, ligands and phase transfer agents should be

soluble in sc-CO_2 to assist in the dissolution process of polymers. Fluorinated polyacrylates, polyethers, and siloxane-based polymers are considered to be sc-CO_2-philic. The sc-fluid drying processes for preparing protein or polysaccharide-containing powders based on these concepts are described in detail by Jovanovic *et al.* [102]. Diez-Municio *et al.* [103] have investigated the impregnation of chitosan with lactulose using supercritical fluids under various operating conditions, in order to improve the solubility of this natural polymer at neutral or basic pH. The highest impregnation yield (8.6%) was obtained for chitosan scaffolds using the following parameters: continuous process, 60 min contact, 14% (v/v) of co-solvent ethanol:water (95:5), depressurization rate 3.3 bar/min, pressure 100 bar, and 100 °C. Under these conditions, the Maillard reaction took place as well. Biodegradable and mucoadhesive PLGA/chitosan microparticles were manufactured by Casettari *et al.* [104] by using scCO_2 with the addition of mPEG and chitosan in the absence of organic solvents, surfactants and crosslinkers. Analytical surface techniques, along with the interaction with mucin, demonstrated the presence of the chitosan (<100 μm) on the surface of the particles.

Chitosan solutions were prepared with acetic acid solution, poured in steel containers and frozen at −20 °C to obtain a hydrogel that was treated in different manners: (1) it was dried with air at 40 °C for 10 h; (2) it was put in a bath of acetone at ambient temperature for 24 h to allow the substitution of water with acetone and was dried with air at 40 °C for 8 h; (3) it was put in a bath of acetone at ambient temperature for 24 h and was dried by sc-CO_2; (4) it was put in a bath of acetone at −20 °C for 24 h and was dried by sc-CO_2 in the high-pressure vessel filled from the bottom with sc-CO_2. When the required pressure and temperature were obtained (200 bar and 35 °C), drying was performed for 4 h with the sc-CO_2 flow rate of about 1 kg/h, that corresponds to a residence time inside the vessel of about 4 min. The depressurization time of 20 min was allocated to bring back the system at atmospheric pressure [105].

When the preference was given to low temperature water substitution followed by supercritical gel drying to prevent the collapse of the chitosan gel, water substitution with acetone was performed at the same temperature of the gel formation (−20 °C for 24 h). Subsequently, sc-CO_2 gel drying was performed at the same processing conditions. In this case, the 3-D shape and the size of samples were preserved, as shown in Figure 3.

The obtained structures present a morphology very similar to the extracellular matrix, *i.e.*, a finely interconnected nano sub-structure, and therefore they can be suitable scaffolds. In fact, this kind of nanometric fibrous network is the ideal environment for cell adhesion and growth for the regeneration of cartilages, skin and bone [105]. The surface properties of biological materials are at the basis of phenomena like cell adhesion, formation of bacterial films, and recognition between biological units. Surface polarity is a major parameter in controlling the adhesion of cells and bacteria, a relevant phenomenon in fields as different as safety of surgical devices, colonization of biomaterials, and sensitivity of biological sensors.

Based on these considerations, supercritically dried aerogels of several polysaccharides have been characterized by Robitzer *et al.* [106]. The nature of the functional groups of the polysaccharide significantly influences the adsorption of N_2 on the surface of the aerogel. Surface area values as high as 570 m^2g^{-1} have been measured. The net enthalpy of adsorption increases with the polarity of the chemical groups of the polymer, in the order: chitin < agar ≤ chitosan < carrageenan < alginic acid/alginate. The surface area and the mesopore distribution of the aerogels depend on the dispersion

of the parent hydrogel and on the behavior of each polymer during the drying treatment. Aerogels retaining the dispersion of the parent hydrogel are mainly macroporous (pores larger than 50 nm) while materials liable to shrink upon solvent exchange form mesoporous structures.

El Kadib *et al.* [107] described a versatile strategy for fabricating highly porous and nanofibrous titania, zirconia, alumina and tin oxide. By taking advantage from the favorable effect of $scCO_2$ drying to avoid the collapse of the transient hybrid material network, all targeted metal oxides were produced, after calcination, as fibrous filaments featuring dual meso- and macro-porous network with surface area ranging from 110 to 310 m^2g^{-1}, as shown in Figures 3 and 4.

Figure 3. The chitosan fibers are replicated by titanium oxide: the SEM image shows the combined chitosan + titania fibers. Reprinted from [107]. Copyright (2011) with permission from Elsevier.

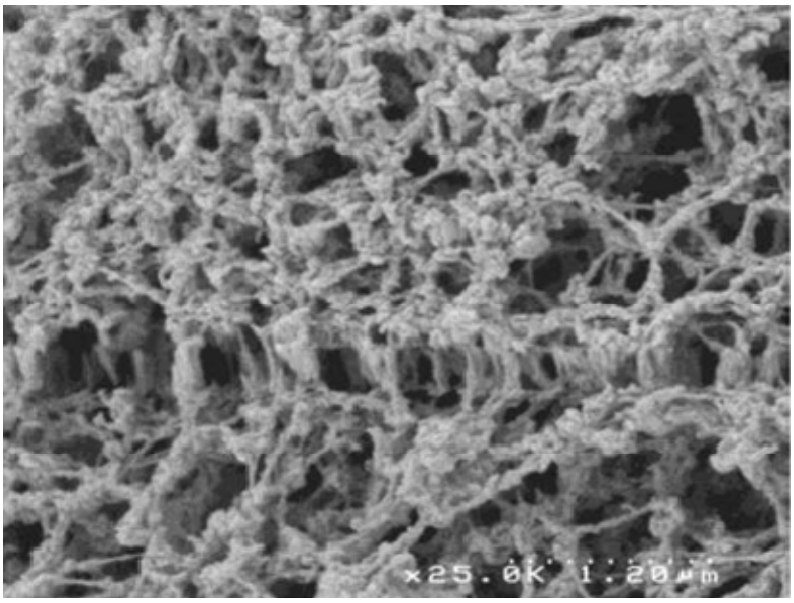

Figure 4. Removal of chitosan leads to pure titanium oxide with filamentous structure. Reprinted from [107]. Copyright (2011) with permission from Elsevier.

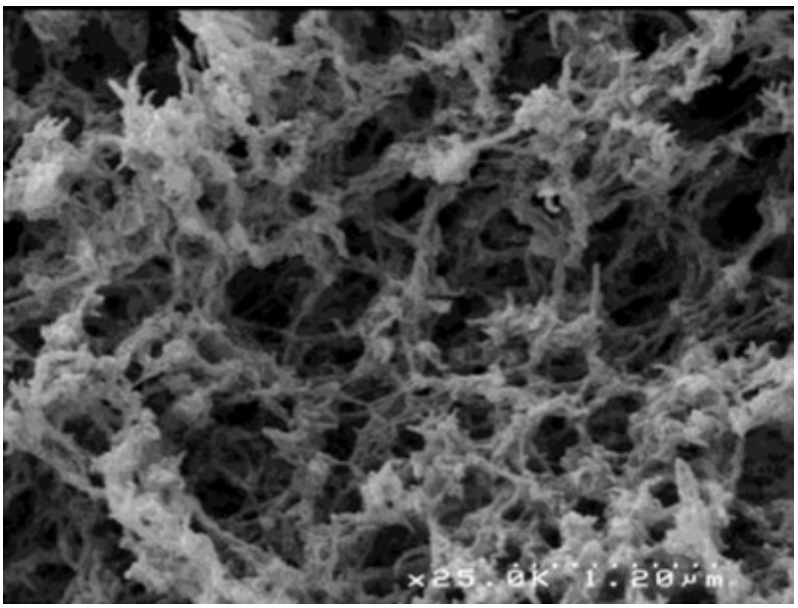

As far as silica is concerned, hydrophobic chitosan+silica hydrogels were prepared by Ayers *et al.* [108]: dried aerogels were exposed to hexamethyldisilazane vapors at 60 °C. After supercritical drying, uncracked monoliths with very little shrinkage were obtained. When exposed to water, said aerogels adsorbed a small amount of liquid at their outer surface, while maintaining their shape. The Brunauer–Emmett–Teller (BET) surface area of said aerogels was very large, 472–750 m^2/g, depending on the ratio chitosan/silica.

In a more elaborated preparation, a solution of chitosan (1%) was mixed with the crosslinker genipin solution (4%) [17]: stirring was continued until the solution turned into a viscous gel. Then the hydrogel was subjected to solvent exchange into acetone thrice to remove water from the structure. After solvent exchange, the chitosan–genipin derivative was placed inside a sealed chamber of the sc-CO_2 extractor at 40 °C and 200 bar. The reaction was left for 2 h and a flow of CO_2 was then applied through the sample in order to replace all the organic solvent with CO_2. The pressure was then released slowly to the atmosphere and the temperature was reduced to 20 °C. The chitosan derivative had BET surface area of 49 m^2/g, with a monolayer volume of 11 cm^3/g. The porosimetry result showed that genipin-crosslinked chitosan scaffold had adequate surface area to provide cell adhesion and proliferation. In fact the osteoblast proliferation on chitosan–genipin scaffolds was assessed using Almar Blue assay and found to be satisfactory considering that the number of cells attached to the genipin-crosslinked chitosan scaffolds after 1, 3, and 7 days of cell culture increased with time thus indicating the suitability of the material for tissue engineering applications [109,110].

The surface of chitin too can be expanded to large values: rapid expansion techniques with sc-CO_2 were used by Salinas-Hernandez *et al.* [111] to form chitin microstructures. Depending on the experimental conditions, they obtained either spherical microparticles with diameters 1.7–5.3 μm with the rapid expansion of sc-solution technique, or continuous microfibers with diameters 11.5–19.3 μm with the rapid expansion into water technique, possibly influenced, in the latter case, by the high forces in the hydrogen bond network of the molecular structure of chitin. It is important to mention that the present method makes it possible to produce much more uniform and thinner nanofibers on a larger scale than the electrospinning process, without using any hazardous chemicals.

6. Conclusion

This bibliographic survey shows the high viability of basic chemical and physical sciences that are promoting the applicability of chitin and chitosan in a number of demanding areas. Just in the most recent years a real interface of existing technologies and chitin science has taken place, and moreover new technologies are emerging in a few scattered articles (hot melt blending, processing, extrusion and stretching [112–115]; foaming [116]; electrofiltration [117]; decrystallization [118]; sonolysis, microfluidization and shearing [119]) that will certainly contribute to the exploitation of renewable chitin-bearing resources.

Acknowledgments

The author is grateful to Marilena Falcone, Central Library, Polytechnic University, Ancona, Italy, for assistance in handling the bibliographic information, and to Maria Weckx for the preparation of the manuscript. This work was not financially supported nor sponsored.

References

1. Muzzarelli, R.A.A. Chitosan composites with inorganics, morphogenetic proteins and stem cells, for bone regeneration. *Carbohydr. Polym.* **2011**, *83*, 1433–1445.
2. Muzzarelli, R.A.A. Chitins and chitosans for the repair of wounded skin, nerve, cartilage and bone. *Carbohydr. Polym.* **2009**, *76*, 167–182.
3. Jayakumar, R.; Chennazhi, K.P.; Srinivasan, S.; Nair, S.V.; Furuike, T.; Tamura, H. Chitin scaffolds in tissue engineering. *Int. J. Mol. Sci.* **2011**, *12*, 1876–1887.
4. Deng, C.; Li, F.F.; Griffith, M.; Ruel, M.; Suuronen, E.J. Application of chitosan-based biomaterials for blood vessel regeneration. *Polym. Org. Chem.* **2010**, *297*, 138–146.
5. Park, B.K.; Kim, M.M. Applications of chitin and its derivatives in biological medicine. *Int. J. Mol. Sci.* **2010**, *11*, 5153–5165.
6. Yang, T.L. Chitin-based materials in tissue engineering: Applications in soft tissue and epithelial organ. *Int. J. Mol. Sci.* **2011**, *12*, 1936–1963.
7. Muzzarelli, R.A.A.; Boudrant, J.; Meyer, D.; Manno, N.; DeMarchis, M.; Paoletti, M.G. Current views on fungal chitin/chitosan, human chitinases, food preservation, glucans, pectins and inulin: A tribute to Henri Braconnot, precursor of the carbohydrate polymers science, on the chitin bicentennial. *Carbohydr. Polym.* **2011**, in press.
8. Morris, G.A.; Kok, M.S.; Harding, S.E.; Adams, G.G. Polysaccharide drug delivery systems based on pectin and chitosan. *Biotechnol. Genet. Eng. Rev.* **2010**, *27*, 257–283.
9. Muzzarelli, R.A.A. Chitosans: New Vectors for Gene Therapy. In *Handbook of Carbohydrate Polymers: Development*, *Properties and Applications*; Ito, R., Matsuo, Y., Eds.; NOVA Publishers: Hauppauge, NY, USA, 2010; pp. 583–604.
10. Chaudhury, A.; Das, S. Recent advancement of chitosan-based nanoparticles for oral controlled delivery of insulin and other therapeutic agents. *AAPS PharmSciTech* **2011**, *12*, 10–20.
11. Petkar, K.C.; Chavhan, S.S.; Agatonovik-Kustrin, S.; Sawant, K.K. Nanostructured materials in drug and gene delivery: A review of the state of the art. *Crit. Rev. Ther. Drug Carrier Syst.* **2011**, *28*, 101–164.
12. Patel, M.P.; Patel, R.R.; Patel, J.K. Chitosan mediated targeted drug delivery system: A review. *J. Pharm. Pharm. Sci.* **2010**, *13*, 536–557.
13. Gupta, B.; Agarwal, R.; Alam, M.S. Textile-based smart wound dressings. *Indian J. Fibre Textile Res.* **2010**, *35*, 174–187.
14. Laurienzo, P. Marine polysaccharides in pharmaceutical applications: An overview. *Mar. Drugs* **2010**, *8*, 2435–2465.
15. Kean, T.; Thanou, M. Biodegradation, biodistribution and safety of chitosan. *Adv. Drug Deliv. Rev.* **2010**, *62*, 3–11.
16. Muzzarelli, R.A.A. Chitin Nanostructures in Living Organisms. In *Chitin Formation and Diagenesis*; Gupta, S.N., Ed.; Springer: New York, NY, USA, 2011.
17. Muzzarelli, R.A.A. Genipin-chitosan hydrogels as biomedical and pharmaceutical aids. *Carbohydr. Polym.* **2009**, *77*, 1–9.

18. Liu, Y.; Shi, X.W.; Kim, E.; Robinson, L.M.; Nye, C.K.; Ghodssi, R.; Rubloff, G.W.; Bentley, W.E.; Payne, G.F. Chitosan to electroaddress biological components in lab-on-a-chip devices. *Carbohydr. Polym.* **2011**, *84*, 704–708.
19. Ngah, W.S.W.; Teong, L.C.; Hanafiah, M.A.K.M. Adsorption of dyes and heavy metal ions by chitosan composites: A review. *Carbohydr. Polym.* **2011**, *83*, 1446–1456.
20. Quignard, F.; Di Renzo, F.; Guibal, E. From natural polysaccharides to materials for catalysis, adsorption, and remediation. *Top. Curr. Chem.* **2010**, *294*, 165–197.
21. Sanchez, C.; Belleville, P.; Popall, M.; Nicole, L. Applications of advanced hybrid organic-inorganic nanomaterials: from laboratory to market. *Chem. Soc. Rev.* **2011**, *40*, 696–753.
22. Jayakumar, R.; Prabaharan, M.; Nair, S.V.; Tamura, H. Novel chitin and chitosan nanofibers in biomedical applications. *Biotechnol. Adv.* **2010**, *28*, 142–150.
23. Liu, Z.H.; Zhang, Z.Y.; Zhou, C.R.; Jiao, Y.P. Hydrophobic modifications of cationic polymers for gene delivery. *Prog. Polym. Sci.* **2010**, *35*, 1144–1162.
24. Muzzarelli, R.A.A. Nanochitins and Nanochitosans, Paving the Way to Eco-Friendly and Energy-Saving Exploitation of Marine Resources. In *Comprehensive Polymer Science*, 2nd ed.; Hoefer, R., Ed.; Elsevier: Amsterdam, the Netherlands, 2011; Volume 10.
25. Zhang, J.L.; Xia, W.S.; Liu, P.; Cheng, Q.Y.; Tahirou, T.; Gu, W.X.; Li, B. Chitosan modification and pharmaceutical/biomedical applications. *Mar. Drugs* **2010**, *8*, 1962–1987.
26. Kumari, A.; Yadav, S.K.; Yadav, S.C. Biodegradable polymeric nanoparticles based drug delivery systems. *Colloids Surf. B* **2010**, *75*, 1–18.
27. Muzzarelli, R.A.A. Chitins and chitosans as immunoadjuvants and non-allergenic drug carriers. *Mar. Drugs* **2010**, *8*, 292–312.
28. Baldrick, P. The safety of chitosan as a pharmaceutical excipient. *Regul. Toxicol. Pharmacol.* **2010**, *56*, 290–299.
29. Kose, R.; Kondo, T. Favorable 3D-network formation of chitin nanofibers dispersed in water prepared using aqueous counter collision. *Fiber* **2011**, *67*, 91–95.
30. Ifuku, S.; Nogi, M.; Abe, K.; Yoshioka, M.; Morimoto, M.; Saimoto, H.; Yano, H. Preparation of chitin nanofibers with a uniform width as alpha-chitin from crab shells. *Biomacromolecules* **2009**, *10*, 1584–1588.
31. Ifuku, S.; Nogi, M.; Yoshioka, M.; Morimoto, M.; Yano, H.; Saimoto, H. Fibrillation of dried chitin into 10–20 nm nanofibers by a simple grinding method under acidic conditions. *Carbohydr. Polym.* **2010**, *81*, 134–139.
32. Shams, M.I.; Ifuku, S.; Nogi, M.; Oku, T.; Yano, H. Fabrication of optically transparent chitin nanocomposites. *Appl. Phys. A* **2011**, *102*, 325–331.
33. Ifuku, S.; Morooka, S.; Nakagaito, A.N.; Morimoto, M.; Saimoto, H. Preparation and characterization of optically transparent chitin nanofiber/(meth)acrylic resin composites. *Green Chem.* **2011**, *13*, 1708–1711.
34. Ifuku, S.; Morooka, S.; Morimoto, M.; Saimoto, H. Acetylation of chitin nanofibers and their transparent nanocomposite films. *Biomacromolecules* **2010**, *11*, 1326–1330.
35. Fan, Y.M.; Saito, T.; Isogai, A. Preparation of chitin nanofibers from squid pen beta-chitin by simple mechanical treatment under acid conditions. *Biomacromolecules* **2008**, *9*, 1919–1923.

36. Liu, D.G.; Wu, Q.L.; Chang, P.R.; Gao, G.Z. Self-assembled liquid crystal film from mechanically defibrillated chitosan nanofibers. *Carbohydr. Polym.* **2011**, *84*, 686–689.
37. Liu, D.G.; Chang, P.R.; Chen, M.D.; Wu, Q.L. Chitosan colloidal suspension composed of mechanically disassembled nanofibers. *J. Colloid Interface Sci.* **2010**, *354*, 637–643.
38. Watthanaphanit, A.; Supaphol, P.; Tamura, H.; Tokura, S.; Rujiravanit, R. Wet-spun alginate/chitosan whiskers nanocomposite fibers: Preparation, characterization and release characteristic of the whiskers. *Carbohydr. Polym.* **2010**, *79*, 738–746.
39. Fan, Y.M.; Saito, T.; Isogai, A. Individual chitin nano-whiskers prepared from partially deacetylated alpha-chitin by fibril surface cationization. *Carbohydr. Polym.* **2010**, *79*, 1046–1051.
40. Ifuku, S.; Nomura, R.; Morimoto, M.; Saimoto, H. Preparation of chitin nanofibers from mushrooms. *Materials* **2011**, *4*, 1417–1425.
41. Muzzarelli, R.A.A.; Morganti, P.; Morganti, G.; Palombo, P.; Palombo, M.; Biagini, G.; Mattioli-Belmonte, M.; Giantomassi, F.; Orlandi, F.; Muzzarelli, C. Chitin nanofibrils with chitosan glycolate composites as wound medicaments. *Carbohydr. Polym.* **2007**, *70*, 274–284.
42. Han, B.; Shi, X.L.; Xiao, J.Q.; Zhang, Y.; Chu, X.H.; Gu, J.Y.; Tan, J.J.; Gu, Z.Z.; Ding, Y.T. Influence of chitosan nanofiber scaffold on porcine endogenous retroviral expression and infectivity in pig hepatocytes. *World J. Gastroenterol.* **2011**, *17*, 2774–2780.
43. Ma, H.Y.; Burger, C.; Hsiao, B.S.; Chu, B. Ultrafine polysaccharide nanofibrous membranes for water purification. *Biomacromolecules* **2011**, *12*, 970–976.
44. Tzoumaki, M.V.; Moschakis, T.; Kiosseoglou, V.; Biliaderis, C.G. Oil-in-water emulsions stabilized by chitin nanocrystal particles. *Food Hydrocoll.* **2011**, *25*, 1521–1529.
45. Huang, C.; Chen, R.; Ke, Q.F.; Morsi, Y.; Zhang, K.H.; Mo, X.M. Electrospun collagen-chitosan-polyurethane nanofibrous scaffolds for tissue engineered tubular grafts. *Colloids Surf. B* **2011**, *82*, 307–315.
46. Hariraksapitak, P.; Supaphol, P. Preparation and properties of alpha-chitin-whisker-reinforced hyaluronan-gelatin nanocomposite scaffolds. *J. Appl. Polym. Sci.* **2010**, *117*, 3406–3418.
47. Yerlikaya, F.; Aktas, Y.; Capan, Y. LC-UV determination of melatonin from chitosan nanoparticles. *Chromatographia* **2010**, *71*, 967–970.
48. Hafner, A.; Lovric, J.; Voinovich, D.; Filipovic-Grcic, J. Melatonin-loaded lecithin/chitosan nanoparticles: Physicochemical characterisation and permeability through Caco-2 cell monolayers. *Int. J. Pharm.* **2009**, *381*, 205–213.
49. Kofuji, K.; Nakamura, M.; Isobe, T.; Murata, Y.; Kawashima, S. Stabilization of alpha-lipoic acid by complex formation with chitosan. *Food Chem.* **2008**, *109*, 167–171.
50. Chang, P.R.; Jian, R.J.; Yu, J.G.; Ma, X.F. Starch-based composites reinforced with novel chitin nanoparticles. *Carbohydr. Polym*. **2010**, *80*, 420–425.
51. Azeredo, H.M.C.; Mattoso, L.H.C.; Avena-Bustillos, R.J.; Ceotto, G.; Munford, M.L.; Wood, D.; McHugh, T.H. Nanocellulose reinforced chitosan composite films as affected by nanofiller loading and plasticizer content. *J. Food Sci.* **2010**, *75*, N1–N7.
52. Junkasem, J.; Rujiravanit, R.; Supaphol, P. Fabrication of alpha-chitin whisker-reinforced poly(vinyl alcohol) nanocomposite nanofibres by electrospinning. *Nanotechnology* **2006**, *17*, 4519–4528.

53. Li, X.X.; Li, X.Y.; Ke, B.L.; Shi, X.W.; Du, Y.M. Cooperative performance of chitin whisker and rectorite fillers on chitosan films. *Carbohydr. Polym.* **2011**, *85*, 747–752.
54. Ezhova, Z.A.; Koval, E.M.; Zakharov, N.A.; Kalinnikov, V.T. Synthesis and physicochemical characterization of nanocrystalline chitosan-containing calcium carbonate apatites. *Russ. J. Inorg. Chem.* **2011**, *56*, 841–846.
55. Rizvi, R.; Cochrane, B.; Naguib, H.; Lee, P.C. Fabrication and characterization of melt-blended polylactide-chitin composites and their foams. *J. Cell. Plast.* **2011**, *47*, 282–299.
56. Nirmala, R.; Il, B.W.; Navamathavan, R.; El-Newehy, M.H.; Kim, H.Y. Preparation and characterizations of anisotropic chitosan nanofibers via electrospinning. *Macromol. Res.* **2011**, *19*, 345–350.
57. Cooper, A.; Bhattarai, N.; Kievit, F.M.; Rossol, M.; Zhang, M.Q. Electrospinning of chitosan derivative nanofibers with structural stability in an aqueous environment. *Phys. Chem. Chem. Phys.* **2011**, *13*, 9969–9972.
58. Jacobs, V.; Patanaik, A.; Anandjiwala, R.D.; Maaza, M. Optimization of Electrospinning Parameters for Chitosan Nanofibres. *Curr. Nanosci.* **2011**, *7*, 396–401.
59. Muzzarelli, R.A.A. Potential of chitin/chitosan-bearing materials for uranium recovery: An interdisciplinary review. *Carbohydr. Polym.* **2011**, *84*, 54–63.
60. Nirmala, R.; Navamathavan, R.; Kang, H.S.; El-Newehy, M.H.; Kim, H.Y. Preparation of polyamide-6/chitosan composite nanofibers by a single solvent system via electrospinning for biomedical applications. *Colloids Surf. B* **2011**, *83*, 173–178.
61. Nirmala, R.; Navamathavan, R.; El-Newehy, M.H.; Kim, H.Y. Preparation and electrical characterization of polyamide-6/chitosan composite nanofibers via electrospinning. *Mater. Lett.* **2011**, *65*, 493–496.
62. Zhang, H.T.; Han, J.; Xue, Y.; Nie, H.L.; Zhu, L.M.; Branford-White, C.J. Surface Modification of Electrospun Nylon Nanofiber Based Dye Affinity Membrane and Its Application to Papain Adsorption. In *Proceedings of 3rd International Conference on Bioinformatics and Biomedical Engineering*, Beijing, China, 11–13 June 2009; Volume 1, pp. 955–958.
63. Hussain, A.; Collins, G.; Cho, C.H. Electrospun Chitosan-Based Nanofiber Scaffolds for Cardiac Tissue Engineering Applications. In *Proceedings of 2010 IEEE 36th Annual Northeast Bioengineering Conference*, New York, NY, USA, 26–28 March 2010; pp. 62–63.
64. Cynthia, W.; Shital, P.; Rui, C.; Owida, A.; Morsi, Y. Biomimetic electrospun gelatin-chitosan polyurethane for heart valve leaflets. *J. Mech. Med. Biol.* **2010**, *10*, 563–576.
65. Xie, D.M.; Huang, H.M.; Blackwood, K.; MacNeil, S. A novel route for the production of chitosan/polylactide-co-glycolide) graft copolymers for electrospinning. *Biomed. Mater.* **2011**, *5*, 159–167.
66. Skotak, M.; Leonov, A.P.; Larsen, G.; Noriega, S.; Subramanian, A. Biocompatible and biodegradable ultrafine fibrillar scaffold materials for tissue engineering by facile grafting of L-lactide onto chitosan. *Biomacromolecules* **2008**, *9*, 1902–1908.
67. Klossner, R.R.; Queen, H.A.; Coughlin, A.J.; Krause, W.E. Correlation of chitosan's rheological properties and its ability to electrospin. *Biomacromolecules* **2008**, *9*, 2947–2953.

68. Ziani, K.; Henrist, C.; Jerome, C.; Aqil, A.; Mate, J.I.; Cloots, R. Effect of nonionic surfactant and acidity on chitosan nanofibers with different molecular weights. *Carbohydr. Polym.* **2011**, *83*, 470–476.
69. Chen, H.L.; Huang, J.; Yu, J.H.; Liu, S.Y.; Gu, P. Electrospun chitosan-*graft*-poly (epsilon-caprolactone)/poly(epsilon-caprolactone) cationic nanofibrous mats as potential scaffolds for skin tissue engineering. *Int. J. Biol. Macromol.* **2011**, *48*, 13–19.
70. Shalumon, K.T.; Anulekha, K.H.; Chennazhi, K.P.; Tamura, H.; Nair, S.V.; Jayakumar, R. Fabrication of chitosan/poly(caprolactone) nanofibrous scaffold for bone and skin tissue engineering. *Int. J. Biol. Macromol.* **2011**, *48*, 571–576.
71. Feng, Z.Q.; Leach, M.K.; Chu, X.H.; Wang, Y.C.; Tian, T.A.; Shi, X.L.; Ding, Y.T.; Gu, Z.Z. Electrospun chitosan nanofibers for hepatocyte culture. *J. Biomed. Nanotechnol.* **2010**, *6*, 658–666.
72. Meng, Z.X.; Zheng, W.; Li, L.; Zheng, Y.F. Fabrication, characterization and *in vitro* drug release behavior of electrospun PLGA/chitosan nanofibrous scaffold. *Mater. Chem. Phys.* **2011**, *125*, 606–611.
73. Qian, Y.F.; Zhang, K.H.; Chen, F.; Ke, Q.F.; Mo, X.M. Cross-linking of gelatin and chitosan complex nanofibers for tissue-engineering scaffolds. *J. Biomater. Sci. Polym. Ed.* **2011**, *22*, 1099–1113.
74. Zhang, K.H.; Qian, Y.F.; Wang, H.S.; Fan, L.P.; Huang, C.; Mo, X.M. Electrospun silk fibroin-hydroxybutyl chitosan nanofibrous scaffolds to biomimic extracellular matrix. *J. Biomater. Sci. Polym. Ed.* **2011**, *22*, 1069–1082.
75. Almodovar, J.; Kipper, M.J. Coating electrospun chitosan nanofibers with polyelectrolyte multilayers using the polysaccharides heparin and *N*,*N*,*N*-trimethyl chitosan. *Macromol. Biosci.* **2010**, *11*, 72–76.
76. Yang, D.Z.; Yu, K.; Ai, Y.F.; Zhen, H.P.; Nie, J.; Kennedy, J.F. The mineralization of electrospun chitosan/poly(vinyl alcohol) nanofibrous membranes. *Carbohydr. Polym.* **2010**, *84*, 990–996.
77. Espindola-Gonzalez, A.; Martinez-Hernandez, A.L.; Fernandez-Escobar, F.; Castano, V.M.; Brostow, W.; Datashvili, T.; Velasco-Santos, C. Natural-synthetic hybrid polymers developed via electrospinning: the effect of PET in chitosan/starch system. *Int. J. Mol. Sci.* **2010**, *12*, 1908–1920.
78. Kim, M.Y.; Lee, J. Chitosan fibrous 3D networks prepared by freeze drying. *Carbohydr. Polym.* **2011**, *84*, 1329–1336.
79. Seo, H.; Matsumoto, H.; Hara, S.; Minagawa, M.; Tanioka, A.; Yako, H.; Yamagata, Y.; Inoue, K. Preparation of polysaccharide nanofiber fabrics by electrospray deposition: Additive effects of polyethylene oxide. *Polym. J.* **2005**, *37*, 391–398.
80. Horzum, N.; Boyaci, E.; Eroglu, A.E.; Shahwan, T.; Demir, M.M. Sorption efficiency of chitosan nanofibers toward metal ions at low concentrations. *Biomacromolecules* **2010**, *11*, 3301–3308.
81. Zhuang, X.P.; Li, Z.; Kang, W.M.; Cheng, B.W. Electrospun antibacterial chitosan/poly(vinyl alcohol) nanofibers containing silver nanoparticles. *New Mater. Adv. Mater.* **2011**, *152–153*, 1333–1336.

82. Su, P.; Wang, C.J.; Yang, X.Y.; Chen, X.Y.; Gao, C.Y.; Feng, X.X.; Chen, J.Y.; Ye, J.A.; Gou, Z.R. Electrospinning of chitosan nanofibers: The favorable effect of metal ions. *Carbohydr. Polym.* **2011**, *84*, 239–246.
83. Uygun, A.; Kiristi, M.; Oksuz, L.; Manolache, S.; Ulusoy, S. Hydrazine plasma modification of chitosan for antibacterial activity and nanofiber applications. *Carbohydr. Res.* **2011**, *346*, 259–265.
84. Huang, C.C.; Lou, C.W.; Lu, C.T.; Huang, S.H.; Chao, C.Y.; Lin, J.H. Evaluation of the Preparation and Biocompatibility of Poly(vinyl alcohol)(PVA)/chitosan Composite Electrospun Membranes. *Adv. Mater. Res.* **2010**, *123–125*, 975–978.
85. Swatloski, R.P.; Spear, S.K.; Holbrey, J.D.; Rogers, R.D. The dissolution of cellulose in ionic liquids. *J. Am. Chem. Soc.* **2002**, *124*, 4974–4975.
86. Xie, H.B.; Zhang, S.B.; Li, S.H. Chitin and chitosan dissolved in ionic liquids as reversible sorbents of CO_2. *Green Chem.* **2006**, *8*, 630–633.
87. Yamazaki, S.; Takegawa, A.; Kaneko, Y.; Kadokawa, J.; Yamagata, M.; Ishikawa, M. Performance of electric double-layer capacitor with acidic cellulose-chitin hybrid gel electrolyte. *J. Electrochem. Soc.* **2010**, *157*, A203–A208.
88. Prasad, K.; Murakami, M.; Kaneko, Y.; Takada, A.; Nakamura, Y.; Kadokawa, J. Weak gel of chitin with ionic liquid, 1-allyl-3-methylimidazolium bromide. *Int. J. Biol. Macromol.* **2009**, *45*, 221–225.
89. Park, T.J.; Jung, Y.J.; Choi, S.W.; Park, H.; Kim, H.; Kim, E.; Lee, S.H.; Kim, J.H. Native chitosan/cellulose composite fibers from an ionic liquid via electrospinning. *Macromol. Res.* **2011**, *19*, 213–215.
90. Takegawa, A.; Murakami, M.; Kaneko, Y.; Kadokawa, J. Preparation of chitin/cellulose composite gels and films with ionic liquids. *Carbohydr. Polym.* **2010**, *79*, 85–90.
91. Wu, Y.; Sasaki, T.; Irie, S.; Sakurai, K. A novel biomass-ionic liquid platform for the utilization of native chitin. *Polymer* **2008**, *49*, 2321–2327.
92. Kadokawa, J.; Takegawa, A.; Mine, S.; Prasad, K. Preparation of chitin nanowhiskers using an ionic liquid and their composite materials with polyvinyl alcohol. *Carbohydr. Polym.* **2011**, *84*, 1408–1412.
93. Wang, W.T.; Zhu, J.; Wang, X.L.; Huang, Y.; Wang, Y.Z. Dissolution behavior of chitin in ionic liquids. *J. Macromol. Sci. B* **2010**, *49*, 528–541.
94. Qin, Y.; Lu, X.M.; Sun, N.; Rogers, R.D. Dissolution or extraction of crustacean shells using ionic liquids to obtain high molecular weight purified chitin and direct production of chitin films and fibers. *Green Chem.* **2010**, *12*, 968–971.
95. Zhou, C.J.; Wu, Q.L. A novel polyacrylamide nanocomposite hydrogel reinforced with natural chitosan nanofibers. *Colloids Surf. B* **2011**, *84*, 155–162.
96. Hua, D.B.; Jiang, J.L.; Kuang, L.J.; Jiang, J.; Zheng, W.; Liang, H.J. Smart chitosan-based stimuli-responsive nanocarriers for the controlled delivery of hydrophobic pharmaceuticals. *Macromolecules* **2011**, *44*, 1298–1302.
97. Chen, A.N.; Luo, Z.P.; Akbulut, M. Ionic liquid mediated auto-templating assembly of $CaCO_3$-chitosan hybrid nanoboxes and nanoframes. *Chem. Commun.* **2011**, *47*, 2312–2314.

98. Lin, J.H.; He, C.Y.; Pang, X.J.; Hu, K.C. Amperometric immunosensor for prostate specific antigen based on gold nanoparticles/ionic liquid/chitosan hybrid film. *Anal. Lett.* **2011**, *44*, 908–921.
99. Safavi, A.; Farjami, F. Electrodeposition of gold-platinum alloy nanoparticles on ionic liquid-chitosan composite film and its application in fabricating an amperometric cholesterol biosensor. *Biosens. Bioelectron.* **2011**, *26*, 2547–2552.
100. Silva, S.S.; Duarte, A.R.C.; Carvalho, A.P.; Mano, J.F.; Reis, R.L. Green processing of porous chitin structures for biomedical applications combining ionic liquids and supercritical fluid technology. *Acta Biomater.* **2011**, *7*, 1166–1172.
101. Moribe, K.; Tozuka, Y.; Yamamoto, K. Supercritical carbon dioxide processing of active pharmaceutical ingredients for polymorphic control and for complex formation. *Adv. Drug Deliv. Rev.* **2008**, *60*, 328–338.
102. Jovanovic, N.; Bouchard, A.; Hofland, G.W.; Witkamp, G.J.; Crommelin, D.J.A.; Jiskoot, W. Stabilization of proteins in dry powder formulations using supercritical fluid technology. *Pharm. Res.* **2004**, *21*, 1955–1969.
103. Diez-Municio, M.; Montilla, A.; Herrero, M.; Olano, A.; Ibanez, E. Supercritical CO_2 impregnation of lactulose on chitosan: A comparison between scaffolds and microspheres form. *J. Supercrit. Fluids* **2011**, *57*, 73–79.
104. Casettari, L.; Castagnino, E.; Stolnik, S.; Lewis, A.; Howdle, S.M.; Illum, L. Surface Characterisation of Bioadhesive PLGA/Chitosan Microparticles Produced by Supercritical Fluid Technology. *Pharm. Res.* **2011**, *28*, 1668–1682.
105. Cardea, S.; Pisanti, P.; Reverchon, E. Generation of chitosan nanoporous structures for tissue engineering applications using a supercritical fluid assisted process. *J. Supercrit. Fluids* **2010**, *54*, 290–295.
106. Robitzer, M.; Tourrette, A.; Horga, R.; Valentin, R.; Boissiere, M.; Devoisselle, J.M.; Di Renzo, F.; Quignard, F. Nitrogen sorption as a tool for the characterisation of polysaccharide aerogels. *Carbohydr. Polym.* **2011**, *85*, 44–53.
107. El Kadib, A.; Molvinger, K.; Cacciaguerra, T.; Bousmina, M.; Brunel, D. Chitosan templated synthesis of porous metal oxide microspheres with filamentary nanostructures. *Microporous Mesoporous Mater.* **2011**, *142*, 301–307.
108. Ayers, M.R.; Hunt A.J. Synthesis and properties of chitosan-silica hybrid aerogels. *J. Non-Cryst. Solids* **2001**, *285*, 123–127.
109. Rinki, K.; Dutta, P.K.; Hunt, A.J.; Clark, J.H.; Macquarrie, D.J. Preparation of chitosan based scaffolds using supercritical carbon dioxide. *Macromol. Symp.* **2009**, *277*, 36–42.
110. Rinki, K.; Dutta, P.K. Physicochemical and biological activity study of genipin-crosslinked chitosan scaffolds prepared by using supercritical carbon dioxide for tissue engineering applications. *Int. J. Biol. Macromol.* **2010**, *46*, 261–266.
111. Salinas-Hernandez, R.; Ruiz-Trevino, F.A.; Ortiz-Estrada, C.H.; Luna-Barcenas, G.; Prokhorov, Y.; Alvarado, J.F.J.; Sanchez, I.C. Chitin microstructure formation by rapid expansion techniques with supercritical carbon dioxide. *Ind. Eng. Chem. Res.* **2009**, *48*, 769–778.
112. Rizvi, R.; Cochrane, B.; Naguib, H.; Lee, P.C. Fabrication and characterization of melt-blended polylactide-chitin composites and their foams. *J. Cell. Plast.* **2011**, *47*, 282–299.

113. Correlo, V.M.; Costa-Pinto, A.R.; Sol, P.; Covas, J.A.; Bhattacharya, M.; Neves, N.M.; Reis, R.L. Melt processing of chitosan-based fibers and fiber-mesh scaffolds for the engineering of connective tissues. *Macromol. Biosci.* **2010**, *10*, 1495–1504.
114. Jeung, S.; Mishra, M.K. Hot melt reactive extrusion of chitosan and poly(acrylic acid). *Int. J. Polym. Mater.* **2011**, *60*, 102–113.
115. Thuaksuban, N.; Nuntanaranont, T.; Pattanachot, W.; Suttapreyasri, S.; Cheung, L.K. Biodegradable polycaprolactone-chitosan three-dimensional scaffolds fabricated by melt stretching and multilayer deposition for bone tissue engineering: Assessment of the physical properties and cellular response. *Biomed. Mater.* **2011**, *6*, 100–116.
116. Ji, C.D.; Annabi, N.; Khademhosseini, A.; Dehghani, F. Fabrication of porous chitosan scaffolds for soft tissue engineering using dense gas CO_2. *Acta Biomater.* **2011**, *7*, 1653–1664.
117. Gozke, G.; Posten, C. Electrofiltration of biopolymers. *Food Eng. Rev.* **2010**, *2*, 131–146.
118. Beckham, G.T.; Crowley, M.F. Examination of the α-chitin structure and decrystallization thermodynamics at the nanoscale. *J. Phys. Chem. B* **2011**, *115*, 4516–4522.
119. Chen, R.H.; Huang, J.R.; Tsai, M.L.; Tseng, L.Z.; Hsu, C.H. Differences in degradation kinetics for sonolysis, microfluidization and shearing treatments of chitosan. *Polym. Int.* **2011**, *60*, 897–902.